the $MoO(cat)(ONR_2)_2$ complexes. Both effects are observed experimentally (Figure 3).

An important implication of the results depicted in Figure 6 is that the variation in electronic properties of the molecules is qualitatively different for molecular structural changes made on the periphery of the ligands vs those made at the metal. In the former case, electronic effects are transmitted through the ligand to the metal with the result that both orbital energies change in the same direction, but with some diminution of the effect at the metal. However, when a change in the metal–coligand bond is made, the metal and catecholate orbital energies change in opposite directions. The result is increased stabilization of the filled catecholate (bonding) orbitals and decreased stabilization of the vacant molybdenum (antibonding) orbitals. Such changes are characteristic of interactions resulting from a chemical bonding process. They can be rationalized, for example, in terms of the theory of hard and soft acids and bases.[32] A change from soft $Et_2NCS_2^-$ to hard Et_2NO^- results in a larger HOMO/LUMO gap and predictable changes in the electrochemical and charge-transfer properties of the molecules.

(32) (a) Parr, R. G.; Pearson, R. G. *J. Am. Chem. Soc.* **1983**, *105*, 7512. (b) Pearson, R. G. *J. Am. Chem. Soc.* **1985**, *107*, 6801.

Acknowledgment. This study is dedicated to the memory of Professor Maxwell J. O'Connor, who initiated the interest of S.F.G. in this research area through example and encouragement. Support of this research by the National Science Foundation (F.A.S., Grant CHE-84-09594) is gratefully acknowledged. L.P.M. was an NSF Research Opportunity Award Participant at Florida Atlantic University, 1985. We thank S. Kint for the FT/IR spectra.

Registry No. I (R = Me), 111159-51-4; I (R = Et), 111159-52-5; I (R = Bz), 111159-54-7; II (R = Me), 111264-40-5; II (R = Et), 111264-37-0; II (R = Bz), 111264-38-1; $MoO(cat)(ONMe_2)_2$, 111159-49-0; $MoO(cat)(ONEt_2)_2$, 111188-97-7; $MoO(cat)(ONBz_2)_2$, 111159-53-6; $MoO(CH_3cat)(ONMe_2)_2$, 111159-55-8; $MoO(CH_3cat)(ONEt_2)_2$, 111159-57-0; $MoO(CH_3cat)(ONBz_2)_2$, 111159-59-2; $MoO(NO_2cat)(ONMe_2)_2$, isomer 1, 111159-50-3; $MoO(NO_2cat)(ONMe_2)_2$, isomer 2, 111264-39-2; $MoO(NO_2cat)(ONEt_2)_2$, 111159-56-9; $MoO(NO_2cat)(ONBz_2)_2$, 111159-58-1; *cis*-$MoO_2(ONMe_2)_2$, 74081-85-9; *cis*-$MoO_2(ONEt_2)_2$, 74081-86-0; *cis*-$MoO_2(ONBz_2)_2$, 74081-87-1; ^{95}Mo, 14392-17-7.

Supplementary Material Available: Table III, listing electrochemical and UV–visible properties of eight $MoO(cat)(S_2CNEt_2)_2$ complexes in acetonitrile (1 page). Ordering information is given on any current masthead page.

Contribution from the Department of Chemistry, Emory University, Atlanta, Georgia 30322, and Biophysics Laboratory and Molecular Pharmacology Laboratory, Division of Biochemistry and Biophysics, Food and Drug Administration, Bethesda, Maryland 20892

HMQC and ^1H and ^{31}P NMR Studies of Platinum Amine Adducts of Tetradeoxyribonucleotides. Relationship between ^{31}P Shift and Potential Hydrogen-Bonding Interactions in pGpG Moieties Cross-Linked by Platinum

Christine Spellmeyer Fouts,[†] Luigi G. Marzilli,*[†] R. Andrew Byrd,[‡] Michael F. Summers,[‡§] Gerald Zon,[‡∥] and Kazuo Shinozuka[‡]

Received December 24, 1986

The dependence of the ^{31}P and ^1H NMR spectra of d(TGGT) on formation of Pt adducts was studied with *cis*-PtA_2Cl_2 compounds, where A_2 = en, $(NH_3)_2$, $(MeNH_2)_2$, tn, Me_2tn, and *N*,*N*-Me_2en. In addition, more limited spectral studies were performed with the following oligonucleotides: d(TTGG), d(GGTT), and d(pGGTT). For all combinations studied, a downfield-shifted ^{31}P signal was observed after treatment with *cis*-PtA_2Cl_2. For d(TGGT)Pt(en) and d(TGGT)-*cis*-$Pt(MeNH_2)_2$, various 2D NMR techniques were selectively employed (NOE, HMQC, HOHAHA, and COSY). For d(TGGT)Pt(en), ^{17}O-labeling studies and 2D NMR methods assigned the downfield ^{31}P NMR signal to GpG, and NOE studies demonstrated that the Pt formed an intrastrand cross-link with the GpG moiety where the G residues were in a head-to-head configuration. 2D NMR methods led to these same conclusions with d(TGGT)-*cis*-$Pt(MeNH_2)_2$. For d(TGGT)Pt(en), the 3′-T was stacked with the 3′-G as evidenced by internucleotide NOEs. There was no indication of such stacking in d(TGGT)-*cis*-$Pt(MeNH_2)_2$. Nevertheless, by a combination of HMQC, HOHAHA, and COSY 2D NMR techniques, we were able to assign completely the ^1H NMR signals for d(TGGT)-*cis*-$Pt(MeNH_2)_2$; this example illustrates the power of the newer 2D methods in signal assignments. The downfield-shifted ^{31}P NMR signal appears to be characteristic of the intrastrand GG cross-link, and no such signal was observed in preliminary studies when the reactants [d(TGGT) + *trans*-$Pt(NH_3)_2Cl_2$] could not form such an adjacent GG cross-link. In contrast, ^1H NMR spectra revealed downfield ^1H signals for the d(TGGT) + *trans*-$Pt(NH_3)_2Cl_2$. Likewise, the shift of the downfield ^{31}P NMR signals of the GpG moiety can be correlated with the potential H-bonding ability of the Pt moiety and of the oligonucleotide. In particular, if there is a phosphate group 5′ to the GpG unit, the ^{31}P NMR signal is further downfield than in analogous species lacking such a group. Furthermore, when the amine group coordinated cis to the 5′-G is capable of H bonding (e.g. NH_2), the GpG ^{31}P signal is further downfield than when this group is cis to amines incapable of H bonding (e.g. Me_2N). Thus, the shift data are consistent with molecular mechanics calculations and recent X-ray structures, which indicate that the 5′-phosphate groups participate in H bonding. A simple correlation between ^1H NMR shifts of the G H8 signals and such H-bonding possibilities was not evident. Temperature and pH variation studies were also performed in selected cases. It is interesting that the downfield ^{31}P NMR signal of the GpG cross-linked moiety was relatively insensitive to such changes whereas ^1H NMR signals were often found to be quite sensitive, in agreement with literature studies.

Introduction

The antitumor agent *cis*-$Pt(NH_3)_2Cl_2$ is one of the most widely used anticancer drugs in the U.S.[1] Considerable evidence indicates that the primary molecular target of the drug is DNA[2] (see footnote 3 for abbreviations) and that the principal type of

[†] Emory University.
[‡] Food and Drug Administration.
[§] Current address: Department of Chemistry, University of Maryland, Baltimore County, Baltimore, MD 21228.
[∥] Current address: Applied Biosystems, Foster City, CA 94404.

(1) (a) Sun, M. *Science* (*Washington, D.C.*) **1983**, *222*, 145. See also: *Platinum Met. Rev.* **1984**, *28*, 157. (b) Pinto, A. L.; Lippard, S. J. *Biochim. Biophys. Acta* **1985**, *780*, 167.
(2) Roberts, J. J. In *Advances in Inorganic Biochemistry*; Eichhorn, G. L., Marzilli, L. G., Eds.; Elsevier North Holland: New York, 1981; Vol. 3, p 273.

0020-1669/88/1327-0366$01.50/0

adduct formed by this drug and the closely analogous species $Pt(en)Cl_2$ is an intrastrand GpG cross-link.[1b,4] Initial ^{31}P NMR spectral studies of DNA treated with antitumor-active Pt drugs revealed the presence of a new signal, ca. 1 ppm downfield from the main DNA signal.[5] This downfield signal is not observed for DNA treated with antitumor-inactive Pt compounds such as *trans*-$Pt(NH_3)_2Cl_2$.[5,6]

The results of DNA studies alone do not provide sufficient evidence for identification of the unusual ^{31}P NMR signal as that for the P in a Pt intrastrand d(GpG) cross-link. The downfield ^{31}P NMR signal was observed with polynucleotides having two adjacent 6-oxopurines (poly(dG)·poly(dC)[5] and poly(I)·poly(C)[7]) when treated with antitumor-active Pt drugs. The signal was not observed when antitumor-inactive Pt drugs were employed, as in the DNA studies.[5] A series of self-complementary oligomers varying in length from 8 to 14 bases with different sequences were treated with Pt drugs.[8] Only when GpG was present in the sequence were downfield ^{31}P NMR signals observed. Separate studies of other small GpG-containing oligomers,[9] both single-stranded and self-complementary, indicate the presence of a Pt intrastrand GpG cross-link. It was determined by ^1H NMR spectroscopy that the G's are linked via N7 to Pt. A summary of this work is available in a recent review.[10] For the sequence d(TCTCGGTCTC),[9g] ^{31}P–^1H decoupling experiments and, for the sequence d(TGGT), HMQC and ^{17}O labeling studies[11] definitely established that the P leading to the downfield signal is in the Pt intrastrand GpG cross-link. NOE experiments with d(TCTCGGTCTC),[9g] poly(I)·poly(C),[7] and d(TGGT)[11] revealed that the adjacent purines of the Pt adduct were in a head-to-head configuration. Molecular mechanics calculations of d(TCTCGGTCTC)-*cis*-$Pt(NH_3)_2$-d(GAGACCGAGA)[12] and X-ray structures of d(pGpG)-*cis*-$Pt(NH_3)_2$[13a] and d(CGG)-*cis*-$Pt(NH_3)_2$[13b] suggest that hydrogen bonding between one amine ligand on Pt and the phosphate group 5′ to the dGpG moiety is an important feature of Pt binding. Also, more recent molecular mechanics calculations on the decamer d(TCTCGGTCTC)-*cis*-$Pt(NH_3)_2$ duplexed with its complement raise the possibility of another hydrogen bond between an amine ligand of Pt to O6 of the 3′-G residue.[14]

It is of some interest that the downfield signal observed with the Pt drugs is dependent on the GC content of the DNA and that it is more readily observed in polymers with less stable duplexes, i.e. in DNA's with low GC content.[6] Since ^{31}P NMR spectroscopy is a structurally informative spectroscopic method that can be applied both to nucleosomes[5] and to oligonucleotides and since the ^{31}P signal position appears to be dependent on the state of the DNA, we have initiated a program aimed at evaluating the relationship between ^{31}P NMR shifts and the nature of the DNA. Recent evidence[1b] suggests that the influence of the Pt adduct on the DNA structure may be an essential feature influencing the activity of the drug.

Previously, we reported preliminary results on the use of ^1H NMR NOE data and on HMQC and ^{17}O methods for the assignments of ^{31}P NMR signals of d(TGGT)Pt(en).[11] In this report, we provide additional information on this adduct under various conditions and extend the study to other tetranucleotides and to additional Pt compounds. In particular, we have been interested in determining if there is a relationship between ^{31}P shift and H-bonding interactions of the NH groups. It may be argued that single-stranded oligonucleotides are not relevant to the anticancer activity of these drugs. However, the nature of the critical lesion on DNA is not known, and this study represents one of the initial steps in the analysis of the much more complex spectra typically found for duplexes.

Experimental Section

Materials. Oligodeoxyribonucleotides were prepared either by the modified phosphotriester method[15] or by the phosphoramidite method.[16] Purity of the oligomers was evaluated by HPLC and ^1H NMR spectroscopy. If necessary, triethylammonium acetate was removed on a 2 × 20 cm G-10 Sephadex gel filtration column (H_2O eluent, 0.5 mL/min). Residual triethylamine was removed by passing the solution over Dowex (Na^+ form). The *cis*-PtA_2Cl_2 compounds (A_2 = en, tn, Me_2tn, *N*,*N*-Me_2en, $(MeNH_2)_2$)[3] were prepared by the method of Dhara.[18] The isomers of $Pt(NH_3)_2Cl_2$ were purchased from Aldrich.

Synthesis of d(pGGTT). *O*-((*p*-Nitrophenyl)ethyl) *O*-methyl *N*,*N*-diisopropylphosphoramidite (^{31}P NMR 145.5 ppm) was synthesized in a manner similar to that described by Uhlmann and Engels.[16d] The product was purified by flash chromatography on silica gel by using 1:1 petroleum ether–EtOAc (v/v) as the eluent. The eluent also contained 2% v/v Et_3N. Acetonitrile solutions of this amidite (0.25 M) and commercially available (Applied Biosystems) *O*-β-cyanoethyl amidite (0.1 M) derivatives of dG and dT were employed for automated (Applied Biosystems Model 380B) synthesis on a 2 × 10 μmol scale according to previously described procedures.[16c] These procedures included demethylation with thiophenol–Et_3N and base deprotection with concentrated

(3) Abbreviations: G = guanine; A = adenine; T = thymine; C = cytosine; en = ethylenediamine; tn = 1,3-propanediamine; Me_2tn = 2,2-dimethyl-1,3-propanediamine; *N*,*N*-Me_2en = *N*,*N*-dimethylethylenediamine; PIPES = piperazine-*N*,*N*′-bis(2-ethanesulfonic acid); HMQC = heteronuclear multiquantum coherence; NOE = nuclear Overhauser enhancement; HOHAHA = homonuclear Hartmann–Hahn; COSY = correlated spectroscopy. Since the charge on Pt adducts is pH dependent, it will not be specified.

(4) (a) Marcelis, A. T. M.; Reedijk, J. *Recl. Trav. Chim. Pays-Bas* **1983**, *102*, 121. (b) Sundquist, W. I.; Lippard, S. J.; Stollar, B. D. *Biochemistry* **1986**, *25*, 1520. (c) Eastman, A. *Biochemistry* **1986**, *25*, 3912. (d) Fichtinger-Schepman, A. M. J.; van der Veer, J.; den Hartog, J. H. J.; Lohman, P.; Reedijk, J. *Biochemistry* **1985**, *24*, 707. (e) Brouwer, J.; van de Putte, P.; Fichtinger-Schepman, A. M. J.; Reedijk, J. *Proc. Natl. Acad. Sci. U.S.A.* **1981**, *78*, 7010.

(5) Wilson, W. D.; Heyl, B. L.; Reddy, R.; Marzilli, L. G. *Inorg. Chem.* **1982**, *21*, 2527. Marzilli, L. G.; Heyl, B. L.; Reily, M. D.; McMurray, C. T.; Wilson, W. D. *FEBS Lett.* **1984**, *176*, 389. Also see ref 9g.

(6) Reily, M. D.; Marzilli, L. G., manuscript in preparation.

(7) Reily, M. D.; Marzilli, L. G. *J. Am. Chem. Soc.* **1985**, *107*, 4916.

(8) Fouts, C. S.; Reily, M. D.; Marzilli, L. G.; Zon, G. Inorg. Chim Acta **1987**, *137*, 1.

(9) (a) Den Hartog, J. H. J.; Altona, C.; Chottard, J.-C.; Girault, J.-P.; Lallemand, J.-Y.; deLeeuw, F. A. A. M.; Marcelis, A. T. M.; Reedijk, J. *Nucleic Acids Res.* **1982**, *10*, 4715. (b) Den Hartog, J. H. J.; Altona, C.; van der Marel, G. A.; Reedijk, J. *Eur. J. Biochem.* **1985**, *147*, 371. (c) Marcelis, A. T. M.; Canters, G. W.; Reedijk, J. *Recl. J. R. Neth. Chem. Soc.* **1981**, *100*, 391. (d) Girault, J.-P.; Chottard, J.-C.; Guittet, E. R.; Lallemand, J.-Y.; Huynh-Dinh, T.; Igolen, J. *Biochem. Biophys. Res. Commun.* **1982**, *109*, 1157. (e) Neuman, J.-M.; Tran-Dinh, S.; Girault, J.-P.; Chottard, J.-C.; Huynh-Dinh, T.; Igolen, J. *Eur. J. Biochem.* **1984**, *141*, 465. (f) den Hartog, J. H. J.; Altona, C.; van Boom, J. H.; van der Marel, G. A.; Haasnoot, C. A. G.; Reedijk, J. *J. Biomol. Struct. Dyn.* **1985**, *2*, 1137. (g) den Hartog, J. H. J.; Altona, C.; van Boom, J. H.; Reedijk, J. *FEBS Lett.* **1984**, *176*, 393. (h) Girault, J.-P.; Chottard, J.-C.; Neumann, J. M.; Tran-Dinh, S.; Huynh-Dinh, T.; Igolen, J. *Nouv. J. Chim.* **1984**, *8*, 7. (i) Van Hemelryck, B.; Guittet, E.; Chottard, G.; Girault, J.-P.; Huynh-Dinh, T.; Lallemand, J.-Y.; Igolen, J.; Chottard, J.-C. *J. Am. Chem. Soc.* **1984**, *106*, 3037. (j) Caradonna, J. P.; Lippard, S. J.; Gait, M. J.; Singh, M. *J. Am. Chem. Soc.* **1982**, *104*, 5793. (k) Inagaki, K.; Kidani, Y. *Inorg. Chim. Acta* **1985**, *106*, 187. (l) Inagaki, K.; Kasuya, K.; Kidani, Y. *Chem. Lett.* **1984**, 171; *Inorg. Chim. Acta* **1984**, *91*, 213. (m) Girault, J.-P.; Chottard, G.; Lallemand, J.-Y.; Chottard, J.-C. *Biochemistry* **1982**, *21*, 1352.

(10) Reedijk, J.; Fichtinger-Schepman, A. M. J.; van Oosterom, A. T.; van de Putte, P. *Struct. Bonding (Berlin)*, in press.

(11) Byrd, R. A.; Summers, M. F.; Zon, G.; Fouts, C. S.; Marzilli, L. G. *J. Am. Chem. Soc.* **1986**, *108*, 504.

(12) Kozelka, J.; Petsko, G. A.; Lippard, S. J.; Quigley, G. J. *J. Am. Chem. Soc.* **1985**, *107*, 1079.

(13) (a) Sherman, S. E.; Gibson, D.; Wang, A. H.-J.; Lippard, S. J. *Science (Washington, D.C.)* **1985**, *230*, 412. (b) Admiraal, G.; van der Veer, J.; de Graff, R. A.; den Hartog, J. H. J.; Reedijk, J. *J. Am. Chem. Soc.* **1987**, *109*, 594.

(14) Kozelka, J.; Petsko, G. A.; Quigley, G. J.; Lippard, S. J. *Inorg. Chem.* **1986**, *25*, 1075.

(15) Gait, M. J.; Singh, M.; Sheppard, R. C.; Edge, M. D.; Greene, A. R.; Heathcliffe, G. R.; Atkinson, T. C.; Newton, C. R.; Markham, A. F. *Nucleic Acids Res.* **1980**, *8*, 1081. Miyoshi, K.; Itakura, K. *Tetrahedron Lett.* **1979**, *28*, 2449. Khorana, H. G. *Science (Washington, D.C.)* **1979**, *203*, 1979.

(16) (a) Stec, W. J.; Zon, G.; Egan, W.; Stec, B. *J. Am. Chem. Soc.* **1984**, *106*, 6077. (b) Broido, M. S.; Zon, G.; James, T. L. *Biochem. Biophys. Res. Commun.* **1984**, *119*, 663. (c) Stec, W. J.; Zon, G.; Egan, W.; Byrd, R. A.; Phillips, L. R.; Gallo, K. A. *J. Org. Chem.* **1985**, *50*, 3908. (d) Uhlmann, E.; Engels, J. *Tetrahedron Lett.* **1986**, *27*, 1023. (e) Zon, G.; Thompson, J. A. *Biochromatography* **1986**, *1*, 22.

(17) Zon, G.; Thompson, J. A. *Biochromatography* **1986**, *1*, 22.

(18) Dhara, S. C. *Indian J. Chem.* **1970**, *8*, 193.

Table I. ^{1}H Chemical Shifts (ppm) of d(TGGT),[a] d(TGGT)Pt(en),[b] and d(TGGT)-*cis*-Pt($MeNH_2$)$_2$[c]

		chem shift								
	Pt complex	H8/H6	CH_3	H1′	H2′	H2″	H3′	H4′	H5′	H5″
5′-T		7.40		5.86						
	Pt(en)	7.46	1.70	5.92	2.10[d]	1.73[d]	4.29	3.80	3.81[e]	3.55[e]
	cis-Pt($MeNH_2$)$_2$	7.55	1.87	6.08	2.37	1.98	4.60	4.01	3.68	3.68
5′-G		7.96		6.05						
	Pt(en)	7.99		6.1[f]	2.68[d]	2.30[d]	5.11	4.12	4.02[e]	3.93[e]
	cis-Pt($MeNH_2$)$_2$	8.35		6.16	2.73	2.34	5.07	4.21	4.05	3.99
3′-G		7.85		6.23						
	Pt(en)	8.96		6.17	2.60[d]	2.63[d]	4.91	4.29	4.07[e]	3.86[e]
	cis-Pt($MeNH_2$)$_2$	8.91		6.17	2.66	2.85	4.95	4.36	4.10	3.95
3′-T		7.52		6.29						
	Pt(en)	7.58	1.66	6.20	2.23[d]	1.65[d]	4.48	4.00	[g]	[g]
	cis-Pt($MeNH_2$)$_2$	7.67	1.82	6.28	2.35	2.04	4.55	4.14	3.95	3.95

[a] Chemical shift assignments based on literature values of other small oligonucleotides.[19-24] [b] Assignments from 2D NOE data collected at 5 °C. See Experimental Section for additional conditions. [c] Assignments from HOHAHA, COSY, and HMQC data at 31 °C. See Experimental Section for additional conditions. Aromatic signals were assigned from 2D NOE data. [d] Based on values for the *cis*-Pt($MeNH_2$)$_2$ adduct. [e] H5′ and H5″ shifts may be interconverted. [f] Broad signal that did not share cross peaks with other signals. [g] Not assigned due to peak overlap.

NH_4OH at 55 °C for 10 h. The crude (*p*-nitrophenyl)ethyl ester product was purified by reversed-phase HPLC[17] using a PRP-1 column (Hamilton, 7 × 305 mm). A 1% min^{-1} gradient of CH_3CN vs 0.1 M triethylammonium acetate (pH 7, TEAA) was employed with the gradient starting at CH_3CN:TEAA = 1:99. The pooled material, which was eluted at ca. 21 min, was taken to dryness in a vacuum centrifuge. The dry material was treated with a mixture of ethylenediamine (1.0 mL), absolute EtOH (1.0 mL), and anhydrous formamide (0.05 mL) at 70 °C for 3 h. The reaction mixture was diluted with TEAA and subjected to HPLC as described above. The material that was eluted at ca. 14 min was taken to dryness in a vacuum centrifuge. A solution of the resultant material in 1 M NaCl was eluted with 1-mL fractions of water from a Bio-Gel P-2 column (15-mL bed volume; Bio-Rad, 200–400 mesh, exclusion limit 1800 Da). Fractions 3 and 4 afforded 172 OD_{260} units of the final product (20% yield based on starting nucleoside).

Instrumentation. ^{1}H NMR spectra were obtained at 361.065 MHz with a Nicolet 360-NB spectrometer equipped with a variable-temperature unit and referenced to $(CH_3)_3SiCH_2CH_2COONa$ (TSP). HMQC, HOHAHA, and 2D NOE experiments were performed on a JEOL GX-400 spectrometer. ^{1}H–^{31}P HMQC data were collected at 21 and 31 °C with the following spectral parameters: accumulated data matrix 1024 × 64 (F1 zero-filled to 128); spectral widths F2(^{1}H) = 1500 Hz and F1(^{31}P) = 500 Hz; Δ delays of 25 ms (21 °C) and 45 ms (31 °C); processed with Gaussian filters of 8 Hz (F1) and 5 Hz (F2). HOHAHA data were collected at 31 °C by using the following spectral parameters: accumulated data matrix 2 × 1024 × 256 (zero-filled in F1 to a final matrix of 1024 × 512); F1 and F2 spectral widths of 3300 Hz; spin-lock mixing time of 60 ms with a spin-lock field of 6 kHz; processing with Gaussian filters of 6 Hz (F1) and 12 Hz (F2). 2D NOE data were collected at 5 °C with the following spectral conditions: 4000-Hz spectral width; 250-μs Δt_1; 128 data points collected in t_1, zero-filled to a final matrix of 512 × 512 points; 300 and 600 ms mixing times; repetition delay 3 s. ^{31}P NMR spectra were obtained at 81.01 MHz with an IBM WP-200SY spectrometer and referenced to trimethyl phosphate (TMP). HPLC analyses to evaluate sample purity and to determine the extent of reaction were performed on a Rainin Rabbit gradient HPLC system with a Hitachi 100-30 spectrophotometer set at 260 nm. Reversed-phase-gradient elutions were employed with a Rainin Microsorb C18 (4.6 mm × 25 cm) column. Eluent A, 0.1 M TEAA, was prepared by dissolving the calculated amount of triethylamine and slightly less than the equivalent amount of glacial acetic acid in HPLC grade water. The solution was passed through a 0.45-μm Millipore filter and the pH adjusted to 7.0 with acetic acid. Eluent B was HPLC-UV grade acetonitrile. Typical gradients were 10–15% B in 20 min at a flow rate of 1.0 mL/min.

Pt Reactions. Unless otherwise indicated, all oligomer solutions were pH 5.5, with 0.010 M bases, D_2O, and 0.001 M EDTA, and reaction solutions were maintained at ca. 21 °C. Reported pH values are uncorrected. The *cis*-PtA_2Cl_2 complexes (A_2 = en, $(NH_3)_2$, $(MeNH_2)_2$) and *trans*-Pt(NH_3)$_2Cl_2$ were added as solids to separate solutions of d(TGGT) to make one Pt per strand. Reaction solutions were incubated at 40 °C until the reaction was complete, as verified by ^{1}H NMR and, in some cases, HPLC (with procedures given above). Reactions for the cis complexes with d(TGGT) were complete within 12–24 h. The reaction of *trans*-Pt(NH_3)$_2Cl_2$ with d(TGGT) was complete in 3 days. Solutions of Pt(Me_2tn)Cl_2, Pt(*N*,*N*-Me_2en)Cl_2, and Pt(tn)Cl_2 were prepared by dissolving 4 mg of the Pt compound in 1 mL of D_2O and heating the mixture to 60 °C until dissolved. An appropriate volume of these Pt solutions was added to solutions of d(TGGT) to give one Pt per strand. Reactions were complete after 36 h for A_2 = Me_2tn and tn, as verified by ^{1}H NMR. For A_2 = *N*,*N*-Me_2en, the reaction was complete after 2 weeks.

Table II. ^{1}H NMR Data (ppm) for d(TGGT) and Its Pt Adducts[a]

	chem shift			
	H8			
Pt compd	3′	5′	H6	H1′
	7.86	7.96	7.51, 7.40	6.21, 6.10, 6.03, 5.86
Pt(en)Cl_2	8.97	8.16	7.64, 7.58	6.28, 6.23, 6.08, 6.04
cis-Pt(NH_3)$_2Cl_2$	9.04	8.25	7.65, 7.57	6.29, 6.21, 6.08, 6.06
Pt(Me_2tn)Cl_2	8.99	8.30	7.66, 7.58	6.31, 6.20, 6.19, 6.09
Pt(tn)Cl_2	8.95	8.37	7.65, 7.57	6.31, 6.18, 6.18, 6.09
cis-Pt($MeNH_2$)$_2Cl_2$	8.98	8.39	7.67, 7.58	6.31, 6.19, 6.19, 6.10
Pt(*N*,*N*-Me_2en)Cl_2	8.80	8.35	7.65, 7.60	6.4–6.0
	9.54	8.46	7.72, 7.55	6.4–6.0
trans-Pt(NH_3)$_2Cl_2$	8.7–8.5		7.7–7.6	6.5–6.1

[a] ^{1}H NMR data in ppm of 0.010 M samples at pH 5.5 in D_2O at ca. 22 °C. H8 signals of the Pt(en) and *cis*-Pt($MeNH_2$)$_2$ adducts were assigned by 2D techniques. Other assignments are based on this study and literature values.[9]

An appropriate amount of freshly prepared solutions of Pt(en)Cl_2 (4 mg/mL and heated to 60 °C until dissolved) was added to separate pH 6.0 solutions of d(TTGG), d(GGTT), and d(pGGTT) to give one Pt per strand. Reactions of d(TTGG), d(GGTT), and d(TAGT) were complete within 24 h (verified by ^{1}H NMR). The reaction of d(pGGTT) with the Pt(en) complex was complete after 18 h (verified by ^{1}H NMR).

cis-Pt($MeNH_2$)$_2Cl_2$ was added as a solution (prepared as described above) to separate pH 6.0 solutions of d(TTGG) and d(GGTT) to make one Pt per strand. Reactions were complete within 24 h as verified by ^{1}H NMR.

Results

^{1}H NMR Spectroscopy. d(TGGT). The numbering scheme of (5′ → 3′) d(TGGT) and the deoxyribose conformations are illustrated in Figure 1. The 8–5 ppm region of the ^{1}H NMR spectrum of d(TGGT) in D_2O at pH 7 and 0.010 M in bases consists of four singlets for each of the nonexchangeable base protons and four doublets of doublets for each of the H1′ protons. Assignments of these resonances, based on literature values of other small oligodeoxyribonucleotides,[9,19-23] are given in Table I.

***cis*-PtA_2Cl_2.** When various Pt complexes with cis Cl leaving ligands were added to solutions of d(TGGT), see Experimental Section for conditions, new sets of signals were observed for each

(19) Wood, D. J.; Hruska, F. E.; Ogilvie, K. K. *Can. J. Chem.* **1974**, *52*, 3353.
(20) Pardi, A.; Walker, R.; Rapoport, H.; Wider, G.; Wüthrich, K. *J. Am. Chem. Soc.* **1983**, *105*, 1652.
(21) Schweizer, M. P.; Broom, A. D.; Ts'o, P. O. P.; Hollis, D. P. *J. Am. Chem. Soc.* **1968**, *90*, 1042.
(22) Danyluk, S. S.; Hruska, F. E. *Biochemistry* **1968**, *7*, 1038.
(23) Den Hartog, J. H. J.; Altona, C.; van der Marel, G. A.; Reedijk, J. *Eur. J. Biochem.* **1985**, *147*, 371.

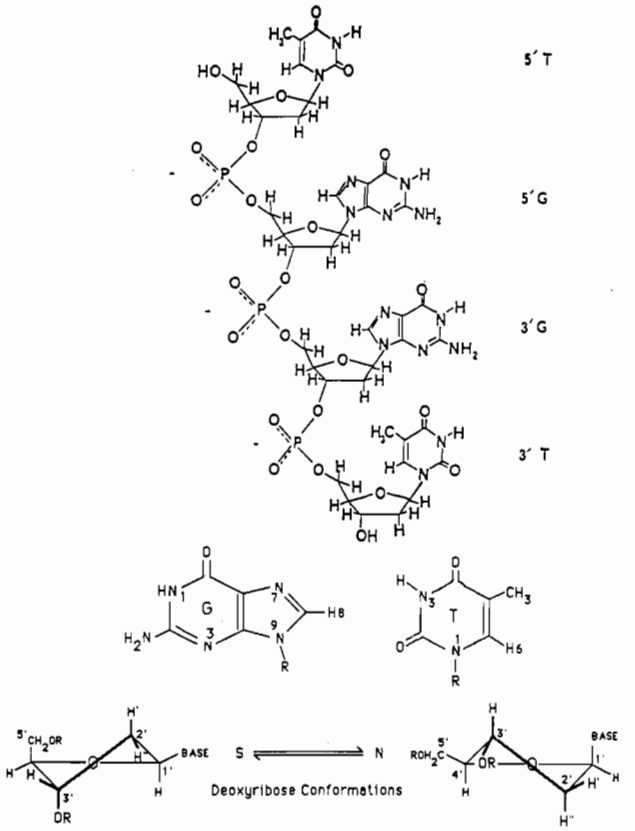

Figure 1. Schematic representation of d(TGGT) with the base and deoxyribose proton-numbering scheme. The S and N conformations of the deoxyribose moieties are also depicted.

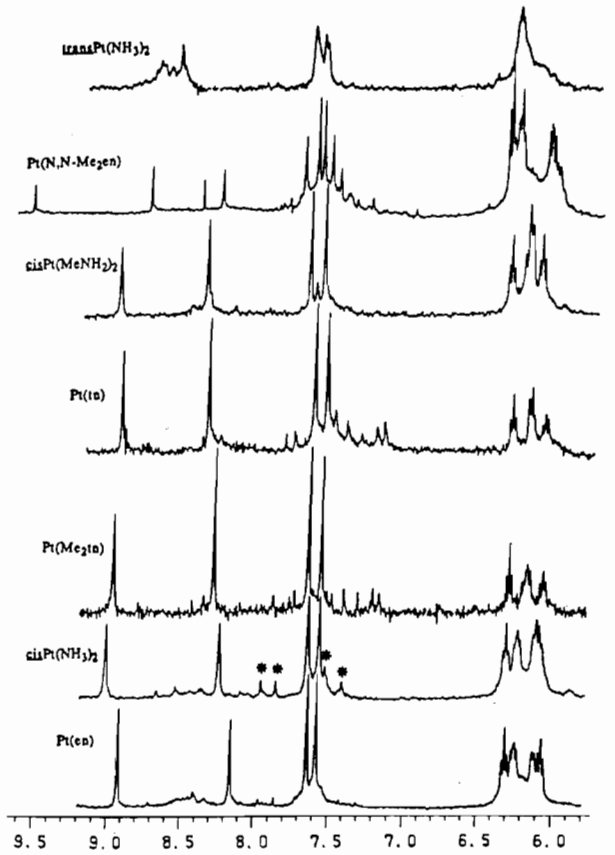

Figure 2. ^{1}H NMR spectra of the base and H1′ region of various d(TGGT) Pt adducts. The small signals in the spectrum of the *cis*-Pt$(NH_3)_2$ adduct are from unreacted d(TGGT), as indicated by an asterisk. See Experimental Section for solution conditions and instrument parameters.

Pt adduct (Table II, Figure 2). For all the symmetric Pt complexes, A_2 = en, *cis*-$(NH_3)_2$, tn, Me_2tn, and *cis*-$(MeNH_2)_2$, one predominant new set of signals was observed, which must correspond to the main signals observed by ^{31}P NMR (see below). However, for the Pt(*N*,*N*-Me_2en)Cl_2 reaction, two new sets of signals were observed in the aromatic region: one set (for adduct A) of G H8 signals, 8.80 and 8.35 ppm, 66% of the H8 signal area; a second set (for adduct B) of G H8 signals, 9.54 and 8.46 ppm, 34% of the signal area.

In all cases, the G H8 signals shifted downfield after reaction of d(TGGT) with the Pt complexes. The 3′-G H8 signals were observed to shift by 0.85 to 1.69 ppm (Table II). The 5′-G H8 signals for the Pt adducts were observed within a 0.30 ppm range. The order of shifting for the 5′-G H8 signals was (most upfield) en < *cis*-$(NH_3)_2$ < Me_2tn < *N*,*N*-Me_2en [A] < tn < *cis*-$(MeNH_2)_2$ < *N*,*N*-Me_2en [B] (Table II). The H6 signals of the T residues were also observed to shift downfield, though only slightly (ca. 0.1 ppm). Of the Pt complexes added, only Pt(en)Cl_2 induced an ^{1}H NMR spectrum in which the H1′ signal of the 5′-G was easily observed at ambient temperature. In all other cases this H1′ signal overlaps other H1′ signals.

Pt(en)Cl_2. A ^{1}H two-dimensional nuclear Overhauser effect (2D NOE) study was performed with a solution of d(TGGT)-Pt(en) (8 mM, D_2O, 0.01 M phosphate buffer, 0.10 M $NaNO_3$, pH 7.1, 5 °C).[11] NOE cross peaks were observed between (a) 5′-G H3′ and 5′-G H8, indicative of an N configuration of the ribose moiety;[9b,e,g] (b) 5′-G H8 and 3′-G H8, indicative of the bases in a head-to-head configuration;[9a,b,e,g] (c) 3′-T H6 and 3′-G H2″, indicating base stacking of the 3′-T and G residues;[24,25] and (d) 5′-T H6 and 5′-T H5′,5″, revealing the higher degree of rotational freedom for the 5′-T residue. No cross peaks were observed between 5′-T and 5′-G, indicating no base stacking between these residues. Assignments based on the HMQC/2D NOE method are provided in Table I.

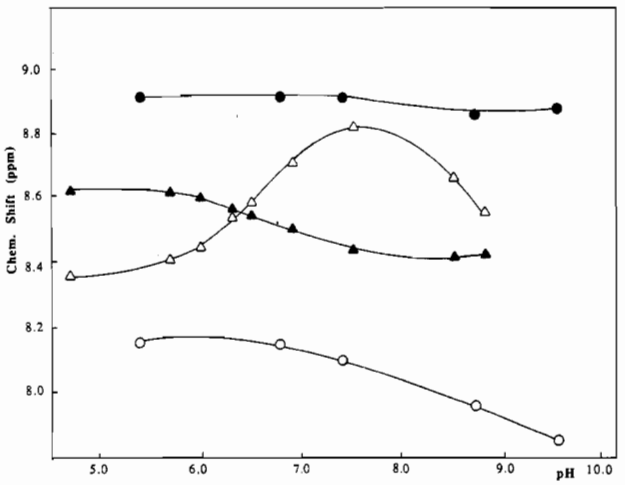

Figure 3. pH dependence of the G H8 signals of d(TGGT)Pt(en) (circles), and d(pGGTT)Pt(en) (triangles). The 5′-G H8 signals for both compounds are represented with open symbols. pH values, uncorrected, were measured before and after recording the ^{1}H NMR spectrum. Chemical shifts were measured from internal TSP at ca. 22 °C.

Addition of $Mg(NO_3)_2$ to 0.10 M to a solution of d(TGGT)-Pt(en) did not change the ^{1}H NMR spectrum. Addition of MeOD to 40%, however, did cause the 5′-G H8 signal to shift downfield from 8.16 to 8.22 ppm. The remaining base and H1′ signals were unaffected. As the pH of the d(TGGT)Pt(en) solution was increased, the 5′-G H8 signal shifted upfield to 7.85 ppm at pH 9.5 (Figure 3). The 5′-G H1′ and the 3′-G H8 signals were unaffected.

(24) Feigon, J.; Denny, W. A.; Leupin, W.; Kearns, D. R. *Biochemistry* **1983**, *22*, 5930. Scheck, R. M.; Boelens, R.; van Boom, J. H.; Kaptein, R. *Biochemistry* **1984**, *23*, 1371.
(25) Wemmer, D. E.; Chou, S.-H.; Hare, D. R.; Reid, B. R. *Biochemistry* **1984**, *23*, 2262.

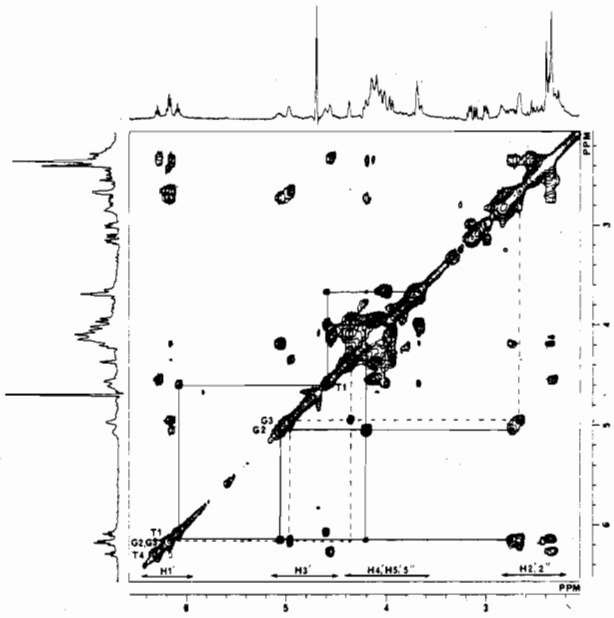

Figure 4. Two-dimensional HOHAHA spectrum of d(TGGT)-*cis*-Pt-$(MeNH_2)_2$ obtained at 31 °C. Partial connectivities are indicated for the G residues below the diagonal and for the 5′-T residue above the diagonal.

***cis*-$Pt(MeNH_2)_2Cl_2$.** 2D NOE measurements were made for solutions of d(TGGT)$Pt(MeNH_2)_2$ (24 mM, D_2O, 0.01 M phosphate buffer, 0.10 M $NaNO_3$, pH 7, 5 °C) prepared by using two mixing times (300 and 600 ms). A strong cross peak between the G H8 protons was observed for both mixing times, similar to that observed for the Pt(en) derivative (vide supra). No additional internucleotide cross peaks were detected for any of the residues. Intranucleotide cross peaks between aromatic base proton resonances (G H8 and T H6) and H2′ and H2″ sugar proton resonances were observed; however, cross peaks between the aromatic proton and other sugar proton resonances were very weak. Thus, although the 2D NOE data were useful for correlating aromatic and sugar protons for a given nucleotide, assignment of the signals to specific nucleotides was not possible.

By combined use of COSY[26] and HOHAHA[27] methods, it is possible to group and assign all ^1H resonances for a given ribose moiety, but not to identify the ribose moiety in the sequence. The HOHAHA experiment is the key element in grouping the proton resonances into J-networks associated with an individual ribose moiety (Figure 4 and supplementary Figure S1). Any ambiguities are resolved via the COSY experiment (supplementary Figure S2).

The complete ^1H assignment is extended to the ^{31}P resonances by reference to the ^1H–^{31}P HMQC data[11] (Figures 5 and 6). At 21 °C, the HMQC spectrum shows very weak correlations for the downfield ^{31}P resonance and overlap of two H3′ resonances; however, it does provide clear correlation to H4′ and H5′,5″ resonances. At 31 °C, the H3′ resonances are all resolved. Weak, but distinguishable, correlations are observed for the downfield ^{31}P resonance. Thus this proton resonance is assigned and concomitantly identifies the 3′-T ribose moiety and the remaining ^1H assignments by reference to the COSY and HOHAHA data. The well-resolved H5′,5″ resonance at 3.68 ppm showed no ^1H–^{31}P correlation (Figure 6), indicating that it must belong to the 5′T

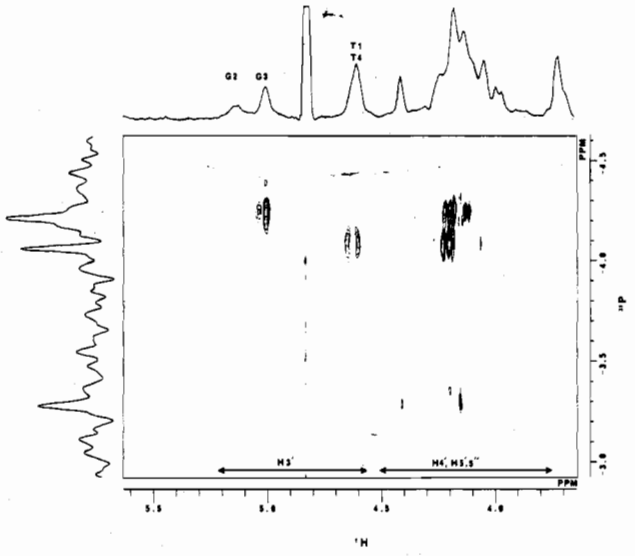

Figure 5. ^1H–^{31}P HMQC spectrum of d(TGGT)-*cis*-Pt$(MeNH_2)_2$ obtained at 20 °C. The normal ^1H and ^{31}P spectra are plotted on the borders of the contour plots. The H3′ resonances are labeled as assigned.

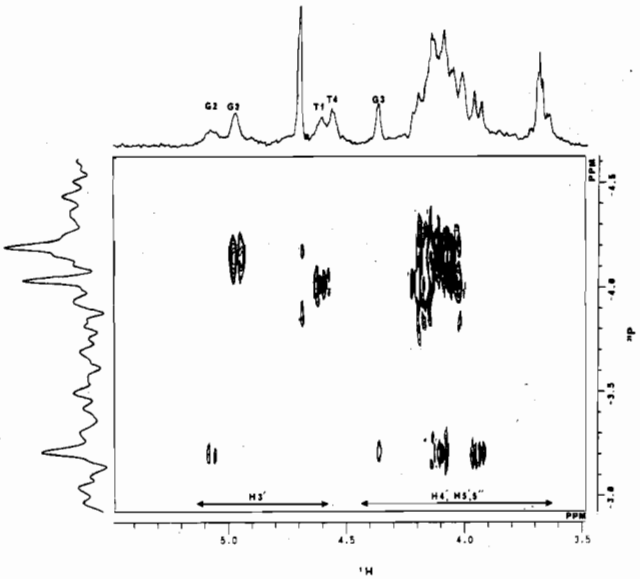

Figure 6. ^1H–^{31}P HMQC spectrum of d(TGGT)-*cis*-Pt$(MeNH_2)_2$ obtained at 31 °C. The normal one-dimensional ^1H and ^{31}P spectra are plotted along the borders of the contour plot. The H3′ resonances are labeled above the ^1H spectrum, corresponding to their assignment. The H4′ resonance of the 3′-G residue is also indicated.

moiety. The remaining 5′-T protons, assigned via the HOHAHA and COSY data, provide identification of the 5′-T H3′ resonance at 4.60 ppm. It is seen to correlate to the −4.04 ppm ^{31}P resonance. There is also a correlation between this ^{31}P resonance and a proton at 4.22 ppm. This proton must be part of the 5′-G ribose, since the HMQC experiment correlates a phosphorus resonance to ^1H resonances of both nucleotides bound to the phosphate. Hence, the −4.04 ppm ^{31}P resonance is assigned as TpG. As above, the remaining 5′-G ^1H assignments are made. A correlation is seen between 5′-G H3′ and the −3.22 ppm ^{31}P resonance, thus assigning it to GpG. The correlation observed between the downfield ^{31}P NMR signal and an additional ^1H signal at 4.36 ppm identifies this signal as part of the 3′-G ribose. The remaining ^1H signals for 3′-G are assigned in the same manner as those for 5′-G. Finally, the 3′-G H3′ proton correlates with the most upfield phosphorus signal, which also correlates with appropriate 3′-T signals, confirming the ^1H signal assignments and identifying the ^{31}P signal as GpT. Assignments of these protons are provided in Table I. The base protons were assigned by correlation of the NOE data with the HOHAHA and COSY results.

(26) Aue, W. P.; Bartholdi, E.; Ernst, R. R. *J. Chem. Phys.* **1976**, *64*, 2229. Bax, A.; Freeman, R. *J. Magn. Reson.* **1981**, *42*, 542. Rance, M.; Sorensen, O. W.; Bodenhausen, G.; Wagner, G.; Ernst, R. R.; Wüthrich, K. *Biochem. Biophys. Res. Commun.* **1983**, *117*, 479.

(27) Braunschweiler, L.; Ernst, R. R. *J. Magn. Reson.* **1983**, *53*, 521. Davis, D. G.; Bax, A. *J. Am. Chem. Soc.* **1985**, *107*, 2820. Davis, D. G.; Bax, A. *J. Am. Chem. Soc.* **1985**, *107*, 7197. Bax, A.; Davis, D. G. *J. Magn. Reson.* **1985**, *65*, 355. Bax, A.; Davis, D. G. In *Advanced Magnetic Resonance Techniques in Systems of High Molecular Complexity*; Nicolai, N., Valensin, G., Eds.; Birkhauser: Basel, in press.

Table III. ^{1}H NMR Data (ppm) for d(TTGG), d(GGTT), and d(pGGTT) and Their Pt Adducts[a]

	chem shift	
	3′ H8, 5′ H8, H2	H6
d(TTGG)	7.85, 7.99	7.61, 7.47
Pt(en)	9.10, 8.03	7.69, 7.61
cis-Pt($MeNH_2$)$_2$	9.06, 8.35	7.66, 7.61
d(GGTT)	7.77, 8.01	7.64, 7.51
Pt(en)	8.45, 8.19	7.67, 7.65
cis-Pt($MeNH_2$)$_2$	8.67, 8.29	7.67, 7.66
d(pGGTT)	7.76, 8.02	7.64, 7.50
Pt(en)	8.59, 8.44	7.66, 7.62
Pt(en)[b]	8.43, 8.82	7.66, 7.62
Pt(*N*,*N*-Me_2en)[c]	(9.52, 8.88, 8.30, 8.28)	7.8–7.4

[a] Solutions at ca. 22 °C, pH 6.0 unless indicated otherwise, 10% D_2O, and referenced to TSP. All solutions 0.010 mM in bases. Tentative assignments based on literature values.[9,19-24] H6 and values in parentheses not assigned. [b] pH 7.6. [c] pH 5.7.

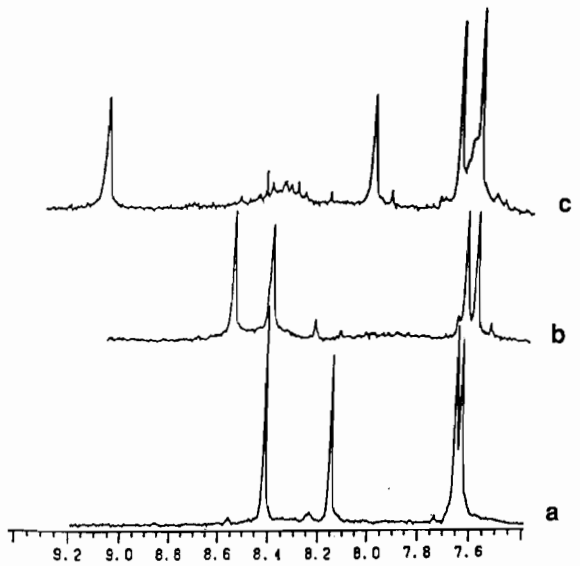

Figure 7. Aromatic region of the ^{1}H NMR spectra of the Pt(en) adducts of (a) d(GGTT), (b) d(pGGTT), and (c) d(TTGG). Solutions were 10 mM in base, D_2O, pH 6.0 (uncorrected), and referenced to internal TSP.

***trans*-Pt(NH_3)$_2$Cl$_2$.** Addition of *trans*-Pt(NH_3)$_2$Cl$_2$ to a solution of d(TGGT) produced broad and numerous peaks in the ^{1}H NMR base and H1′ region (Table II and Figure 2). No distinct signals were observed. This phenomenon was probably due to the inability of the trans complex to form intrastrand cross-links with G residues. Thus interstrand cross-links could be formed, and the number of reaction products produced is considerable.

Analogues of d(TGGT). d(TTGG). The base region of the ^{1}H NMR spectrum of d(TTGG) at pH 6.0 and ca. 22 °C contains four signals (Table III). Reaction with Pt(en)Cl$_2$ gave rise to a new set of signals (Table III and Figure 7). The 3′- and 5′-G H8 signals were observed 0.13 ppm downfield and 0.13 ppm upfield, respectively, of the corresponding G H8 signals of d(TGGT)Pt(en). The 3′-G H8 signal of d(TTGG)-*cis*-Pt($MeNH_2$)$_2$ is observed 0.08 ppm further downfield than the 3′-G H8 signal of d(TGGT)-*cis*-Pt($MeNH_2$)$_2$ (Table III).

d(GGTT). The ^{1}H NMR spectrum of d(GGTT) contains four signals in the 9–7 ppm region (Table III). Addition of Pt(en)Cl$_2$ and *cis*-Pt($MeNH_2$)$_2$Cl$_2$ to separate solutions of d(GGTT) gave rise to new sets of signals (Table III and Figure 7). The 3′-G H8 signals for the Pt(en) and *cis*-Pt($MeNH_2$)$_2$ adducts were observed 0.52 and 0.31 ppm upfield, respectively, to the corresponding adducts of d(TGGT). The 5′-G H8 signal for the Pt(en) adduct was close in value fo that of d(TGGT)Pt(en); this signal for the *cis*-Pt($MeNH_2$)$_2$ adduct, however, was observed 0.10 ppm upfield of that for d(TGGT) isomer.

d(pGGTT). The base region of d(pGGTT) at pH 7.0 consists of two G H8 and two T H6 signals (Table III and supplementary Figure S3). One hour after addition of a solution of Pt(en)Cl$_2$ (pH 5.7), small new H8 signals of about equal intensity, presumably for the two monofunctionally Pt–G(N7) bound species, were observed at 8.36, 8.35, 7.99, and 7.93 ppm. After 2 h, additional signals were observed for the [d(GpG)-*N7*,*N7*]Pt(en) adduct. These signals, at 8.62, 8.36, 7.65, and 7.61 ppm, dominate the spectrum after 12 h. Small signals were observed for the unchanged d(pGGTT) and for the two monofunctionally Pt bound species. The reaction was essentially complete at 18 h. The aromatic regions of the ^{1}H NMR spectra of this reaction are provided in supplementary Figure S3.

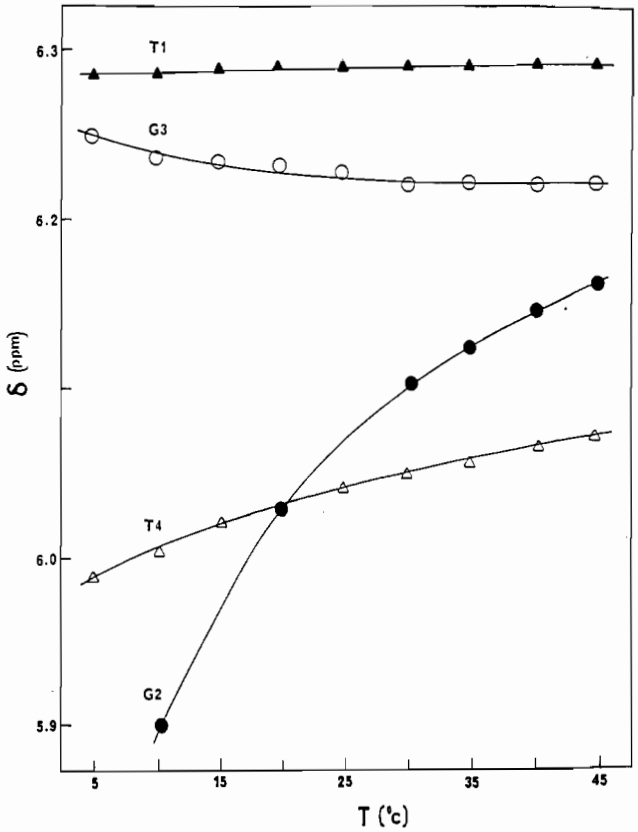

Figure 8. Temperature dependence of the H1′ signals of d(TGGT)Pt(en). Solution was 10 mM in base, D_2O, and pH 5.5. Chemical shifts were measured from internal TSP.

The G H8 signals of d(pGGTT)Pt(en) were observed to shift dramatically over a pH range of 4.7–8.8 (Figure 3). At pH 6.0, the signal at 8.44 ppm began to broaden and continued to broaden up to pH 8.8. This signal shifted downfield from 8.36 ppm at pH 4.7 to 8.82 ppm at pH 7.5. An upfield shift was observed on raising the pH further. The second H8 signal shifted upfield by ca. 0.2 ppm on increasing the pH from 4.7 to 8.8. The former signal can be assigned as the 5′ H8 based on the following: (1) a downfield shift observed on increasing the pH for *cis*-Pt(NH_3)$_2$(5′-GMP)$_2$;[28] (2) a downfield shift for the 5′ H8 signal also observed when the pH of [d(pGG)-*N7*,*N7*]*cis*-Pt(NH_3)$_2$ was increased.[9m] The H8 signals of this compound were tentatively assigned by comparison of deuterium exchange rates of both H8′s.[9m]

The ^{1}H NMR spectrum of d(pGGTT) after treatment with 1 equiv of Pt(*N*,*N*-Me_2en)Cl$_2$ (pH 5.7 and 48 h reaction time) contained numerous signals in the 9–7 ppm region. The T H6 signals (7.8–7.4 ppm) overlapped severely. Four G H8 signals were observed at 9.52, 8.88, 8.30, and 8.28 ppm with several small signals (8.62, 8.44, 8.21, and 8.16 ppm) also apparent.

(28) Chu, G. Y. H.; Mansy, S.; Duncan, R. E.; Tobias, R. S. *J. Am. Chem. Soc.* **1978**, *100*, 593.
(29) Saenger, W. In *Principles of Nucleic Acid Structure*; Cantor, C. R., Ed.; Springer-Verlag: New York, 1984; p 61 and references contained therein.

Temperature Dependence of ^{1}H NMR Spectra. The 5′-G H1′ of d(TGGT)Pt(en) was observed as a doublet ($J_{1'-2'} < 0.5$ Hz and $J_{1'-2''} = 7.36$ Hz at 6.16 ppm at 45 °C) indicative of an N-type ribose conformation.[30] As the temperature is lowered, the doublet shifts upfield and broadens to the base line by 5 °C, with comparatively little shifting of the other H1′ proton resonances (Figure 8 and supplementary Figure S4). This phenomenon has been observed with other small oligomers containing the [d(GG)-*N7*,*N7*]-*cis*-Pt(NH$_3$)$_2$ adduct.[9a,m,23]

The aromatic region of the ^{1}H NMR spectrum of d(TGGT)-Pt(en) also shows an effect due to temperature. The H8 signals of both G residues show a greater temperature dependence than the T H6 signals. The H8 signal of the 3′-G shifts upfield by 0.23 ppm, from 9.08 ppm at 5 °C to 8.85 ppm at 45 °C (supplementary Figures S4 and S5). The 5′-G H8 signal shifts downfield by 0.09 ppm, from 8.06 ppm at 5 °C to 8.15 ppm at 45 °C (supplementary Figure S6). Little change is observed for either of the T H6 signals.

The 3′-G H8 signal of d(TGGT)-*cis*-Pt(MeNH$_2$)$_2$ was observed to shift upfield with increasing temperature (supplementary Figure S5). This signal shifts by 0.15 ppm, from 9.06 ppm at 5 °C to 8.91 ppm at 45 °C, a much smaller effect than for the Pt(en) adduct. The 5′-G H8 signal of d(TGGT)-*cis*-Pt(MeNH$_2$)$_2$ does not exhibit much change in this temperature range (supplementary Figure S6).

Increasing the temperature from 5 to 45 °C shifted the 3′-G H8 signals slightly upfield for both adducts of d(TGGT)Pt(*N*,-*N*-Me$_2$en), (0.02 ppm for adduct A and 0.06 ppm for adduct B (supplementary Figure S5). The 5′-G H8 signal shifted upfield by 0.06 ppm for adduct A and downfield by 0.01 ppm for adduct B on increasing the temperature from 5 to 45 °C (supplementary Figure S6).

Increasing the temperature of the d(GGTT)Pt(en) solution from 5 to 45 °C affected both H8 signals nearly equally with upfield shifts of ca. 0.1 ppm (supplementary Figures S5 and S6). This result contrasts with those for d(TGGT)Pt(en) and d(TGGT)-*cis*-Pt(MeNH$_2$)$_2$, where temperature affected the H8 signals of the 3′- and 5′-G residues differently. For the d(GGTT)Pt(en) analogue, however, there is no 5′-phosphate group on the GpG moiety available for H bonding to the amine ligand.

The effect of temperature on the H8 signals of d(pGGTT)-Pt(en) was investigated at pH 7.6 and 6.0, above and below the pK_a of the 5′-phosphate group (vide infra). From 5 to 45 °C, the 5′-G H8 signals shift upfield by 0.2 and 0.1 ppm at pH 7.6 and at pH 6.0, respectively (supplementary Figure S6). The 3′-G H8 signal, at pH 7.6, shifts slightly downfield (0.02 ppm) over this temperature range (supplementary Figure S5). At pH 6.0, the 3′-G H8 signal was not affected by temperature.

^{31}P NMR Spectroscopy. d(TGGT). Pt(en)Cl$_2$. The synthesis of the three ^{17}O-labeled d(TGGT) oligomers [d(T[^{17}O]GGT), d(TG[^{17}O]GT), and d(TGG[^{17}O]T)] employed the phosphoramidite method[16,17] in which the phosphite ester is oxidized in the presence of water that is ca. 40% H$_2$^{17}O, 40% H$_2$^{18}O, and 20% H$_2$^{16}O. Because adventitious water cannot be totally excluded, the labeled products do not exactly reflect these percentages. The signal of the ^{17}O-labeled P is both diminished in intensity by the quadrupolar ^{17}O nucleus and appears as two signals separated by ca. 0.03 ppm, arising from the ^{16}O and ^{18}O species (the upfield shift is an isotope effect of ^{18}O).[30,31] The latter feature, when resolved, is of greater utility since it is unnecessary to purify reaction products extensively or to follow stringent procedures in ^{31}P NMR signal intensity measurements (such as 90° pulse, 5T_1 relaxation delay, and NOE evaluations). The three ^{17}O-labeled oligomers of d(TGGT) and the Pt(en) adducts were studied by ^{31}P NMR spectroscopy (Table IV).[11] The signal of the ^{17}O-labeled P was easily assigned in each case. The downfield shifted signal (−2.89 ppm at 15 °C) in the Pt(en) adduct is clearly that of the phosphate group between the G residues, an assignment verified by the HMQC/2D NOE method.[11] This method selects only the ^{1}H nuclei of oligomers (H3′, H5′, H5″) that are spin-coupled to ^{31}P and correlates them with the ^{31}P chemical shift. For d(TGGT)Pt(en), each ^{31}P resonance was correlated with the corresponding H3′ resonance of the preceding nucleotide. The downfield ^{31}P signal was also correlated with the 3′-G H5′ and H5″ resonances. Severe overlap for the H5′ and H5″ resonances of 5′-G and 3′-T prevented phosphorus correlations with these ^{1}H resonances.

Table IV. ^{31}P NMR Data (ppm) for ^{17}O-Labeled d(TGGT) and Pt Adducts[a]

	T, °C	chem shift GpG	chem shift TpG, GpT
d(TGGT)[b,c]	25	−4.14	−4.20, −4.09
d(T[^{17}O]GGT)	25	−4.12	(−4.18, −4.21), −4.06
d(TG[^{17}O]GT)	25	(−4.15, −4.18)	−4.21, −4.08
d(TGG[^{17}O]T)	25	−4.13	−4.21, −4.08[d]
d(TGGT)Pt(en)[b,c]	15	−2.88	−4.17, −4.21
d(T[^{17}O]GGT)Pt(en)	15	−2.89	(−4.19, −4.22), −4.26
d(TG[^{17}O]GT)Pt(en)	15	(−2.89, −2.92)	−4.19, −4.23
d(TGG[^{17}O]T)Pt(en)	15	−2.89	−4.19, (−4.23, −4.26)

[a] Values in parentheses are the ^{31}P[^{16}O,^{18}O] signals. All solutions are 0.020 M base, PIPES 10, 10% D$_2$O, and pH 7 except as noted. [b] 0.010 M bases. [c] D$_2$O, no salt. [d] ^{31}P[^{16}O,^{18}O] signal not completely resolved from signal at −4.13 ppm.

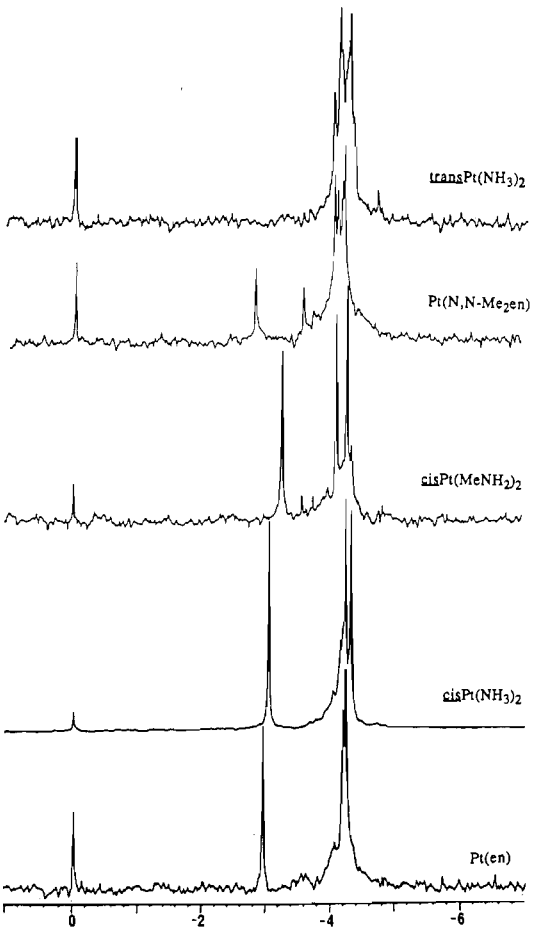

Figure 9. ^{31}P NMR spectra of various Pt adducts of d(TGGT). Solutions were 0.010 M in base, D$_2$O, pH 5.5, and referenced to TMP.

***cis*-PtA$_2$Cl$_2$.** Various d(TGGT) Pt complexes derived from Pt species with cis Cl leaving ligands have ^{31}P NMR spectra with downfield ^{31}P signals in the order of shift as follows: (most downfield) en > *N*,*N*-Me$_2$en [A] > *cis*-(NH$_3$)$_2$ > Me$_2$tn > tn > *cis*-(MeNH$_3$)$_2$ > *N*,*N*-Me$_2$en [B] (Table V and Figure 9). For both Pt(en) and *cis*-Pt(MeNH$_2$)$_2$ adducts of d(TGGT), the downfield ^{31}P signal was assigned to the phosphate group between

(30) Tsai, M.-D. In *Phosphorus-31 NMR*; Gorenstein, D. G., Ed.; Academic: New York, 1984; p 175.
(31) Ts'o, P. O. P.; Kondo, N. S.; Schweizer, M. P.; Hollis, D. P. *Biochemistry* **1969**, *8*, 997. Schweizer, M. P.; Broom, A. D.; Ts'o, P. O. P.; Hollis, D. P. *J. Am. Chem. Soc.* **1968**, *90*, 1042.

Table V. ^{31}P NMR Data (ppm) for d(TGGT) and Its Pt Adducts[a]

A_2	chem shift	
	GpG	TpG, GpT
	−4.18	−4.26, −4.14
en[b,c]	−2.88	−4.17, −4.21
cis-$(NH_3)_2$	−3.02	−4.19, −4.28
Me_2tn	−3.08	(−4.11, −4.29)
tn	−3.09	(−4.09, −4.29)
cis-$(MeNH_2)_2$[b]	−3.22	−4.04, −4.21
N,N-Me_2en	−2.94	(−4.16, −4.21, −4.25, −4.27)
	−3.76	
trans-$(NH_3)_2$		(−3.9 to −4.3, −4.64)

[a] All data collected at 15 °C and at pH 5.5, unless indicated otherwise. Solutions were 0.010 M in base in D_2O. Reference is TMP. Values in parentheses were not assigned. [b] Undecoupled data collected at 25 °C indicate an observed ^1H coupling of 7.8 ± 0.5 Hz. [c] At ca. 25 °C, the GpG signal at −2.95 ppm (pH 7.0) shifted downfield to −2.88 ppm at pH 10.7. Decreasing the pH to 3.5 shifted this signal to −3.01 ppm.

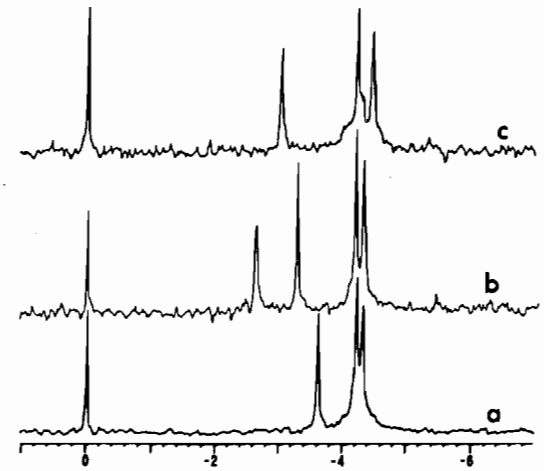

Figure 10. ^{31}P NMR spectra at 25 °C of Pt(en) adducts of (a) d(GGTT), (b) d(pGGTT), and (c) d(TTGG). Solutions were 0.010 M in base, 10% D_2O, pH 6.0 (except for d(pGGTT), pH 5.7), and referenced to TMP.

the G residues by the HMQC method (vide supra). The range of this downfield signal is from −2.88 to −3.76 ppm, relative to TMP. Also consistent with the ^1H NMR results, two downfield signals are observed for d(TGGT)Pt(*N,N*-Me_2en). The downfield signal at −2.94 ppm (adduct A, ca. 60% of downfield ^{31}P signal area) exhibits a typical (ca. −3 ppm) shift observed with this series of Pt complexes (Table V). The signal at −3.76 ppm (adduct B, ca. 40% of downfield signal area) exhibits the smallest downfield shift of the GpG cross-linked adducts. The TpG and GpT signals are affected only slightly by addition of the Pt complexes (Table V and Figure 9).

***trans*-$Pt(NH_3)_2Cl_2$.** After reaction of *trans*-$Pt(NH_3)_2Cl_2$ with d(TGGT), no downfield signal was seen in the ^{31}P NMR spectrum, consisting of several closely spaced signals (Table V and Figure 9).

Analogues of d(TGGT). d(TTGG). The ^{31}P NMR spectrum of d(TTGG) consists of three signals (Table VI). On addition of 1 equiv of $Pt(en)Cl_2$, the characteristic downfield signal is observed at −3.03 ppm (Figure 10). Similarly, addition of *cis*-$Pt(MeNH_2)Cl_2$ gave rise to a ^{31}P NMR signal at −3.38 ppm (Table VI). Although somewhat upfield from those of d(TGGT)PtA_2 adducts (Table II), the signals are consistent with the d(TGGT) results.

d(GGTT). The ^{31}P NMR spectrum of d(GGTT) consists of two signals coincident at −4.19 ppm and a third signal at −4.27 ppm (Table VI). Addition of $Pt(en)Cl_2$ to a solution of d(GGTT) gave rise to a downfield GpG signal at −3.60 ppm (Figure 10). The signal is further upfield than for Pt(en) adducts of oligomers with a phosphate group 5′ to the −GpG− residue. For d(GGTT)-*cis*-$Pt(MeNH_2)_2$, this signal occurs at −3.45 ppm (Table VI). For this tetramer, with no 5′-phosphate group available for H-bonding to the amine of Pt, the GpG signal of the Pt(en) adduct is *upfield* of that for the *cis*-$Pt(MeNH_2)_2$ adduct.

Table VI. ^{31}P NMR Data for d(TTGG), d(GGTT), and d(pGGTT) and Their Pt Adducts[a]

	chem shift, ppm			obsd
	−GpG	−TpG−	TpT−	coupling, Hz
d(TTGG)	−4.11	−4.28	−4.35	
Pt(en)	−3.03	(−4.21	−4.44)	7.6
cis-$Pt(MeNH_2)_2$	−3.38	(−4.22	−4.35)	
	chem shift, ppm			obsd
	GpG−	−GpT−	−TpT	coupling, Hz
d(GGTT)	−4.19	−4.19	−4.27	
Pt(en)	−3.60	(−4.21	−4.30)	4.9
cis-$Pt(MeNH_2)_2$	−3.45	(−4.18	−4.24)	6.8
	chem shift, ppm			obsd
	−GpG−	−GpT−	−Tpt	pG− coupling, Hz
d(pGGTT)	(−4.19	−4.21	−4.28)	−2.56
Pt(en)[b]	−3.34	−4.23	−4.34	−2.74 5.9
Pt(en)[c]	−3.03	−4.26	−4.36	0.35
Pt(en)[d]	−3.08	−4.19	−4.33	0.68
	chem shift, ppm			
	−GpG−	CpG−		$J_{3'H-P}$, Hz
d(GG)[e]				
cis-$Pt(NH_3)_2$	−3.35			7.0
d(CGG)[f]				
cis-$Pt(NH_3)_2$	−2.6	−4.1		7.6

[a] Solutions at pH 6.0, in D_2O, 25 °C, and 0.010 M in base unless indicated otherwise. Values in parentheses are not assigned. Other assignments were based on previous data with TGGT and literature values.[33] Observed couplings are accurate to ±0.5 Hz. [b] pH 5.7. [c] pH 7.6. [d] pH 9.3. [e] From ref 9a. Data collected at 27 °C. Solution was 0.040 M in base, D_2O, and pH 6.5. [f] From ref 9b. Data collected at ca. 20 °C, 0.024 M in base, D_2O, and pH 7.0.

d(pGGTT). For a solution of d(pGGTT) at pH 6.0 and ambient temperature, the ^{31}P spectrum consists of one signal at −2.56 ppm, typical of a phosphate monoester,[30,31] and three phosphodiester signals (Table VI). Addition of a solution of $Pt(en)Cl_2$ gives rise to signals at −2.74, −3.34, −4.23, and −4.34 ppm (pH 5.7). These signals can be assigned as pG, [(GpG)-*N7,N7*]Pt(en), GpT, and TpT, respectively, based on results in this and other studies.[9,19-23] The signal at −3.34 ppm is slightly pH dependent and moves downfield to −3.03 ppm at pH 7.6; increasing the pH further results in a slight upfield shift to −3.08 ppm at pH 9.3. A downfield shift from −3.01 ppm at pH 3.5 to −2.88 ppm at pH 10.7 for the GpG signal of d(TGGT)Pt(en) was also observed. The signal for the 5′-phosphate group is also pH dependent and shifts from −2.89 ppm at pH 4.7 to 0.68 ppm at pH 9.3 (supplementary Figure S7). This signal begins to broaden at pH 5.7 and is extremely broad by pH 6.6. Increasing the pH of the solution further results in a sharpening of this signal as it continues to shift downfield. The pK_a of this phosphate monoester, determined from both ^1H NMR data (3′-G H8 signal) and from ^{31}P NMR data (GpG signal), was found to be 6.9 ± 0.1 by a published method[32] and is close to the value of ca. 7.1 reported for d(pGG)-*cis*-$Pt(NH_3)_2$.[9m]

Temperature Dependence. The ca. −3 ppm ^{31}P signal shifts upfield slightly on increasing the temperature in three of the d(TGGT)PtA_2 adducts studied (A_2 = en, *cis*-$(NH_3)_2$, and *cis*-$(MeNH_2)_2$) (supplementary Figure S8). This upfield shifting is largest for d(TGGT)Pt(en), and the downfield signal is observed to shift from −2.88 ppm at 15 °C to −3.03 ppm at 60 °C. With temperature increase, the GpT and TpG ^{31}P signals shift downfield to common values of −4.13 ppm at 45 °C and −4.05 ppm at 60 °C. The temperature effects for d(TGGT)-*cis*-$Pt(NH_3)_2$, d(TGGT)-*cis*-$Pt(MeNH_2)_2$, and both adducts of d(TGGT)Pt(*N,N*-Me_2en) are smaller. The GpG signal of the *cis*-$Pt(NH_3)_2$

(32) Reily, M. D.; Marzilli, L. G. *J. Am. Chem. Soc.* **1986**, *108*, 6785.

adduct shifts from −2.96 ppm at 5 °C to −3.06 ppm at 60 °C. The GpG signal of the *cis*-Pt($MeNH_2$)$_2$ adduct shifts from −3.22 ppm at 15 °C to −3.30 ppm at 60 °C.

The GpG signal of d(GGTT)Pt(en) was also observed to shift upfield from −3.46 at 5 °C to −3.58 ppm at 45 °C. No further shifting of this signal was observed above 45 °C.

A pH 6.0, the GpG signal of d(pGGTT)Pt(en) does not shift (<0.05 ppm) from 5 to 45 °C (supplementary Figure S8). The remaining signals shift upfield by 0.25 ppm (pG), and downfield by 0.25 (GpT) and 0.17 ppm (TpT) over this range.

^{31}P Coupling Constants. Observed proton–phosphorus couplings of the GpG ^{31}P signal were measured for selected Pt adducts (Table VI). In each case the downfield signal appeared as a broad doublet. The values found for d(TGGT)Pt(en), d(TGGT)-*cis*-Pt($MeNH_2$)$_2$, and d(TTGG)Pt(en) were similar.

Discussion

The dominant factors influencing changes in ^{31}P chemical shift values of phosphodiesters in a given solvent are the ROPOR′ bond and torsional angles.[33] Typically, the ^{31}P signal in B-type DNA occurs within a few tenths of a ppm of −4.2 ppm (relative to TMP). Denaturation of the DNA,[34] treatment with H^+,[35] or addition of many metal ions[5] usually does not shift the signal of native DNA outside this range. The phosphate groups are removed from the base by several bonds, and thus inductive effects are insufficient to cause appreciable changes in the ^{31}P signal. For example, *trans*-Pt(NH_3)$_2$Cl$_2$ and [Pt(diethylenetriamine)Cl]$^+$ species do not alter the shifts greatly for B-type DNA.[5,6]

Appreciable changes are observed for Z-DNA[34] and for DNA treated with known intercalators[36] as well as with cationic porphyrins that may act as intercalators.[37] Likewise, single- and double-stranded oligonucleotides have signals at ca. −4.2 ppm that change with the addition of reagents in a manner similar to those of native DNA.[37,38]

A new downfield ^{31}P signal or a downfield shift of the main ^{31}P signal in DNA indicates an increase in the unwinding angle characterized by changes in R–O–P–OR torsion angles.[33] The downfield ^{31}P chemical shift (ca. −3 ppm) observed for GpG-containing oligomers treated with Pt drugs[8,9a,b,g,11] thus implies that when the Pt drug binds to N7 of adjacent G residues, an extension of the conformation about the diester group between the G residues occurs. The effects of direct interactions of R′OP(O)$_2$OR$^-$ groups with Pt(II) on ^{31}P shift are not known. Recently, it was shown that the effect on a monoester, $ROPO_3^{2-}$, was an approximate 3.5 ppm downfield shift.[39]

Studies with *cis*-Pt(NH_3)$_2$[d(GG)-*N7,N7*][9a] and *cis*-Pt(NH_3)$_2$[d(CGG)-*N7,N7*][9b] (abbreviated as d(GG)-*cis*-Pt(NH_3)$_2$ and d(CGG)-*cis*-Pt(NH_3)$_2$) revealed that the GpG ^{31}P signal for the former, with no phosphate group or base 5′ to the GpG group, was ca. 0.7 ppm upfield from that of the latter, which contains a base and a phosphate group 5′ to the GpG moiety. This difference in chemical shift and molecular mechanics calculations,[12,14] suggesting that the phosphate group 5′ to the GpG moiety could accept an H bond from the amine, led us to investigate whether this GpG ^{31}P NMR signal could be correlated with the expected H-bonding abilities of the amine and the oligonucleotide. The presence of NH groups on the Pt enhances anticancer activity.[10]

The GpG ^{31}P NMR signals (^{31}P NMR signal of unplatinated d(GG) is at ca. −4.1 ppm[40]) of d(GG)-*cis*-Pt(NH_3)$_2$[9a] and d(CGG)-*cis*-Pt(NH_3)$_2$[9b] were observed at −3.35 and −2.6 ppm, respectively. A comparison of the GpG ^{31}P NMR signals of Pt(en) adducts of d(TGGT), d(TTGG), d(GGTT), and d(pGGTT) (Tables V and VI) reveals a similar relationship in chemical shift; i.e., the GpG ^{31}P signal is shifted further downfield for those adducts in which H bonding of a 5′-phosphate group to an amine of Pt is possible. For d(TGGT)Pt(en) and d(TTGG)Pt(en), we observed GpG signals at −2.88 and −3.03 ppm, respectively. For d(GGTT)Pt(en) the GpG signal, at −3.60 ppm, is even further upfield than that of d(GG)-*cis*-Pt(NH_3)$_2$. It was expected that the monoprotonated form of d(pGGTT)Pt(en) would behave analogously to d(TGGT)Pt(en) and d(TTGG)Pt(en). However, the position of the GpG signal at −3.34 ppm (pH 6.0, Table VI) is similar to that of d(GG)-*cis*-Pt(NH_3)$_2$, implying that little H bonding is occurring at this pH, perhaps because of greater rotational freedom of the phosphate group or because the proton withdraws too much electron density from the phosphate group. In the dianion form (pH 9.3), however, the GpG signal is shifted further downfield to −3.08 ppm (supplementary Figure S7) as expected if H bonding strengthens with increased negative charge on the phosphate group. Thus it appears that H bonding of a 5′-phosphate group to an amine on Pt influences the ^{31}P NMR chemical shift of the d(GpG)Pt(en) moiety by extending the diester conformation further as reflected by the increased downfield GpG chemical shift.

By varying the bulk of the amine group of Pt, we observed differences in chemical shift that can be correlated with expected subtle changes in the strength of H bonding to the 5′-phosphate group. In one of the two possible adducts formed on treatment of d(TGGT) with Pt(*N,N*-Me_2en)Cl$_2$, the methyl groups are cis to the 3′-G residue, allowing 5′-phosphate group H bonding to protons of the amine. For this adduct, designated as A, a ^{31}P chemical shift value of the GpG signal similar to that of d(TGGT)Pt(en) is expected. The adduct in which the methyl groups are cis to the 5′-G, eliminating the possibility of H bonding to the 5′-phosphate group, is designated as B. A relatively small downfield shift for the GpG signal is expected for this adduct. On this basis, the major adduct formed on treatment of d(TGGT) with Pt(*N,N*-Me_2en)Cl$_2$ is assigned to structure A. For the series of d(TGGT)-*cis*-PtA_2 adducts in this study, the GpG signal (Table V) was shifted further downfield with A_2 ligands of decreasing bulk cis to the 5′-G with the following order: (most downfield) en > *N,N*-Me_2en [A] > *cis*-(NH_3)$_2$ > Me_2tn > tn > *cis*-($MeNH_2$)$_2$ > *N,N*-Me_2en [B]. This order suggests that H bonding of the 5′-phosphate to the amine promotes an extended phosphate diester conformation.

The effect of bulk of the amine ligand on the GpG ^{31}P chemical shift observed for d(TGGT)-*cis*-PtA_2 adducts was also found for d(TTGG)-*cis*-PtA_2 adducts. The GpG signal of d(TTGG)Pt(en) was more deshielded than that for d(TTGG)-*cis*-Pt($MeNH_2$)$_2$ (Table VI). Thus, for both d(TGGT)-*cis*-PtA_2 and d(TTGG)-*cis*-PtA_2, the most deshielded signals occurred for the Pt(en) adducts with signals at −3.03 and −2.88 ppm, respectively. Less deshielded signals, −3.22 ppm for d(TGGT)-*cis*-Pt($MeNH_2$)$_2$ and −3.38 ppm for d(TTGG)-*cis*-Pt($MeNH_2$)$_2$, were observed when the amine was more bulky, suggesting less favorable H-bonding interactions.

Relatively less deshielded signals were found when either no proton was present on the amine or no 5′-phosphate group (to the GpG moiety) was present on the tetramer, as in d(TGGT)Pt(*N,N*-Me_2en) [B], −3.76 ppm (Table V), or d(GGTT)Pt(en) and d(GGTT)-*cis*-Pt($MeNH_2$)$_2$, −3.60 and −3.45 ppm, respectively (Table VI). Interestingly, for these d(GGTT)Pt adducts, the ^{31}P GpG signal for the Pt(en) adduct is upfield of that for the *cis*-Pt($MeNH_2$)$_2$ adduct.

It is notable that the GpG ^{31}P shifts for the Pt adducts of the four oligomers studied from ca. 5 to 50 °C are not very temperature dependent (supplementary Figure S8). This finding suggests that similar H-bonding interactions and phosphate diester

(33) Gorenstein, D. G. In *Phosphorus-31 NMR*; Gorenstein, D. G., Ed.; Academic: New York, 1984; p 7.
(34) Chen, C. W.; Cohen, J. S. In *Phosphorus-31 NMR*; Gorenstein, D. G., Ed.; Academic: New York, 1984; p 233. The Pt(diethylenetriamine) adduct of poly(dGC)$_2$ promotes the Z form of DNA under appropriate conditions and hence can modify the ^{31}P NMR spectrum. See: Ushay, H. M.; Santella, R.; Cardonna, J.; Grunberger, O.; Lippard, S. J. *Nucleic Acids Res.* **1982**, *10*, 3573.
(35) Banville, D. L.; Marzilli, L. G.; Wilson, W. D. *Biochemistry* **1986**, *25*, 7393.
(36) Wilson, W. D.; Jones, R. L. *Nucleic Acids Res.* **1982**, *10*, 1399.
(37) Marzilli, L. G.; Banville, D. L.; Zon, G.; Wilson, W. D. *J. Am. Chem. Soc.* **1986**, *108*, 4188.
(38) Wilson, W. D.; Jones, R. L.; Zon, G.; Scott, E. V.; Banville, D. L.; Marzilli, L. G. *J. Am. Chem. Soc.* **1986**, *108*, 7113.
(39) Reily, M. D.; Marzilli, L. G. *J. Am. Chem. Soc.* **1987**, *109*, 8299.
(40) Cheng, D. M.; Kan, L.-S.; Iuorno, V. L.; Ts'o, P. O. P. *Biopolymers* **1984**, *23*, 575.

conformations persist over a large temperature range. In contrast, the ^{31}P shift for GpG in d(CGG)-*cis*-Pt$(NH_3)_2$ at 10 °C is ca. −2.7 ppm, and the signal moved to higher field with increasing temperature.[9b] This temperature dependence was attributed to CG stacking. Above 45 °C, stacking was eliminated and the ^{31}P chemical shift of ca. −2.9 ppm agrees well with d(TGGT)Pt(en) at lower temperature where the 5′-T is not stacked.

Proton–phosphorus coupling constants can provide information on the conformation about the C(5′)–O(5′)–P–O(3′)–C(3′) bonds. Due to the flexibility about these bonds and the number of conformations possible, however, detailed information is difficult to obtain. For d(GG)-*cis*-Pt$(NH_3)_2$[9a] and d(CGG)-*cis*-Pt$(NH_3)_2$[9b], $J_{3'H-P}$ values have been reported as 7.0 and 7.6 Hz, respectively. $J_{5'H-P}$ and $J_{5''H-P}$ are reported to be less than 4 Hz and $J_{4'H-P}$ is reported to be less than 3 Hz for both oligomers. Overlap in the ^1H spectra for the H3′, H4′, and H5′,5″ regions prevented determination of the J_{H-P} values in this study. From the large values obtained from the ^{31}P NMR spectra, these couplings are tentatively assigned to $J_{3'H-P}$ (Table VI).

Since the ^{31}P and ^1H chemical shifts of GpG and G H8 signals (vide infra) and $J_{3'H-P}$ assignments of d(TGGT)-*cis*-PtA_2, d(TTGG)-*cis*-Pt(en), and d(GGTT)-*cis*-Pt$(MeNH_2)_2$ (7.8 Hz for both d(TGGT) complexes, 7.6 Hz for d(TTGG)Pt(en), and 6.8 Hz for d(GGTT)-*cis*-Pt$(MeNH_2)_2$; Tables V and VI) are similar within experimental error to the data reported for d(CGG)-*cis*-Pt$(NH_3)_2$ (7.6 Hz),[9b] the conformation along C(5′)–O(5′)PO(3′)–C(3′) is probably similar for these species, i.e. a trans conformation along both β (the C(4′)–C(5′)–O(5′)–P torsion angle) and ϵ (the C(4′)–C(3′)–O(3′)–P torsion angle).

The $^1H-^{31}P$ correlations observed in the HMQC experiments verify the value of $J_{3'H-P}$ of ca. 7.5–8.0 Hz for d(TGGT)-*cis*-Pt$(MeNH_2)_2$: however, the low intensity of the correlation peaks of the GpG moiety indicates changes in coupling constants between riboses within the molecule. These are most likely changes in the intraribose $J_{3'H-2'H}$, $J_{3'H-2''H}$, and $J_{3'H-4'H}$ coupling constants, which are different for the S and N forms of the ribose. The presence of larger trans H–H couplings in the N form[29] could lead to the type of weak correlations observed in the HMQC experiment.[11,41]

The chemical shifts of the aromatic ^1H NMR signals (G H8) are influenced by two major types of effects: (1) through-bond effects, due to coordination of the bases to the Pt drugs, can induce large downfield movements of H8 signals; (2) through-space effects, dependent primarily on factors such as ring currents of adjacent bases and relative orientation of the bound G residues, can exhibit a greater diversity of influence on H8 chemical shifts. Furthermore, other factors such as proximity of phosphate groups can influence H8 shifts. Downfield shifted purine H8 signals of GpG-containing oligomers after treatment with Pt drugs have been observed with a number of mononucleotides[9m,42] and oligonucleotides.[9a-i,m] For mononucleotides, the through-bond effect of Pt bound to N7 on the H8 signal of a purine is observed on the formation of the 1:1 *cis*-Pt$(NH_3)_2$ complexes, *cis*-Pt$(NH_3)_2$(5′-GMP-*N7*)(H_2O) and *cis*-Pt$(NH_3)_2$(5′-IMP-*N7*)(H_2O). Complexation shifts the H8 signals downfield from the free ligand by 0.67 and 0.70 ppm, respectively.[42] Ring current shielding effects have been observed on binding of the second nucleotide to form *cis*-Pt$(NH_3)_2$(5′-GMP-*N7*)$_2$ and *cis*-Pt$(NH_3)_2$(5′-IMP-*N7*)$_2$, where the H8 signals are shifted downfield from the free ligand by only 0.48 and 0.58 ppm, respectively.[42] The formation of the bis complexes *cis*-Pt$(NH_3)_2$[d(5′-GMP-*N7*)$_2$] and *cis*-Pt$(NH_3)_2$[d(3′-GMP-*N7*)$_2$], gives rise to H8 signals shifted downfield from the free ligand by ca. 0.4 ppm.[9b] Free rotation of the nucleotides about the N7–Pt bonds permits these complexes to adopt configurations with minimal steric strain and optimal electronic interactions.[43,44] A single H8 signal is observed for these probably head-to-tail complexes.[9b]

In the [d(GpG)-*N7,N7*]-*cis*-PtA_2 containing oligomers, the G moieties are tethered by a phosphate group and cannot rotate freely about the N7–Pt bonds. NOE studies[9b,e,g] of these oligomers show cross peaks between the 5′-G H8 and its H3′ indicating that the base is in an anti conformation. Additionally, the head-to-head conformation of the G residues was confirmed by the observation of NOE cross peaks between 3′- and 5′-G H8 signals. This conformation is also observed for d(TGGT)Pt(en)[11] and d(TGGT)-*cis*-Pt$(MeNH_2)_2$. For these head-to-head complexes, because of the relative orientation of the bound G residues, the 5′- and 3′-G H8's experience different anisotropic effects from the neighboring bases, resulting in different observed chemical shifts. These H8 protons also have different relationships to the ribose groups.

Comparison of deuterium exchange rates of the H8's of d(GG)-*cis*-Pt$(NH_3)_2$ tentatively assigned the furthest downfield signal as the 3′-G H8.[9m] NOE studies combined with decoupling experiments have assigned the furthest downfield signal to the 3′-G H8 for the *cis*-Pt$(NH_3)_2$ adducts of d(CGG),[9b] d(ATGG),[9c] and d(TCTCGGTCTC).[9g] For both Pt(en) and *cis*-Pt$(MeNH_2)_2$ adducts of d(TGGT), 2D NMR techniques also assigned the furthest downfield signal to the 3′-G H8. Thus, the data obtained for d(TGGT) Pt adducts are consistent with those for related Pt species.

In platinated single-stranded oligomers, the 5′-G H8 signal is shifted downfield by ca. 0.3 ppm and the 3′-G H8 signal is shifted downfield by ca. 1.0 ppm.[9b] For example, the 5′-G H8 signals for d(GG)-*cis*-Pt$(NH_3)_2$[9a] and d(CGG)-*cis*-Pt$(NH_3)_2$[9b] appear at 8.27 and 8.24 ppm, respectively, while the 3′-G H8 signals for these oligomers appear at 8.57 and 8.92 ppm, respectively. This difference has also been observed for longer oligomers such as d(TCTCGGTCTC)-*cis*-Pt$(NH_3)_2$.[9f] Interestingly, when the latter was duplexed with its complement, d(GAGACCGAGA), the 5′-G H8 signal is further downfield than the 3′-G H8 signal.

Except for *N,N*-Me_2en [A], the 5′-G H8 signals of the d(TGGT)PtA_2 complexes are affected by the bulk of A, in much the same way as are the GpG ^{31}P NMR signals, as follows: (most upfield) en < *cis*-$(NH_3)_2$ < Me_2tn < *N,N*-Me_2en [A] < tn < *cis*-$(MeNH_2)_2$ < *N,N*-Me_2en [B] (Table II). The assignments of the H8 signals of the Pt(*N,N*-Me_2en) adducts are based on the relative size of the H8 signals. However, increasing the bulk of the amine group cis to the 5′-G tends to shift the 5′-G H8 signal further downfield. This effect on H8 of increasing amine bulk is also apparent for the d(GGTT) and d(TTGG) adducts, where the 5′ H8 for the Pt(en) adduct is upfield from that for the *cis*-$(MeNH_2)_2$ adduct (Table III).

Ring current effects are also apparent from the 5′-G H8 chemical shift values given in Tables II and III. The chemical shift values of d(TTGG)-*cis*-PtA_2 adducts are upfield from the Pt adducts of d(TGGT) and d(GGTT), suggesting that the 5′-G H8 signal is shielded by the 5′-T and that the additional 5′-base in the d(TTGG) adduct influences this shielding.

The 5′-G H8 signal of d(pGGTT)Pt(en) is further downfield than first expected from the d(TGGT)Pt(en) data (Table III). Studies with 5′-mononucleotides[45] indicate that phosphate group deprotonation (ca. pH 6) induces a downfield shift of the purine H8 and pyrimidine H6 signals. this "wrong way" shift has been attributed to deshielding of the H8 signals by the phosphate group.[45] In particular, the 5′ H8 signal of d(pGG)-*cis*-Pt$(NH_3)_2$ shifted from ca. 8.45 ppm at pH 3 to ca. 8.80 ppm at pH 8.[9m] This shift agrees well with the pH titration of d(pGGTT)Pt(en) (Figure 3), where the signal shifted from 8.40 ppm at pH 4.7 to 8.81 ppm at pH 7.5. Thus, the influence of a 5′-phosphate monoester on the 5′-G H8 signal is different from that of a 5′-phosphate diester.

The chemical shifts of the 3′-G H8 signals of the Pt complexes appear to be predominantly dependent on base sequence in the following order: (most upfield) d(GGTT)-*cis*-PtA_2, d(pGGTT)-*cis*-PtA_2 < d(TGGT)-*cis*-PtA_2 < d(TTGG)-*cis*-PtA_2

(41) Byrd, R. A.; Egan, W.; Summers, M. F.; Bax, A. *Carbohydr. Res.*, in press.
(42) Marcelis, A. T. M.; Erkelens, C.; Reedijk, J. *Inorg. Chim. Acta* **1984**, *91*, 129.
(43) Marcelis, A. T. M.; van der Veer, J. L.; Zwetsloot, J. C. M.; Reedijk, J. *Inorg. Chim. Acta* **1983**, *78*, 195.
(44) Cramer, R. E.; Dahlstrom, P. L. *J. Am. Chem. Soc.* **1979**, *101*, 3679.
(45) Martin, R. B. *Acc. Chem. Res.* **1985**, *18*, 32.

< d(TGGT)Pt(*N*,*N*-Me_2en) [B] (Tables II and III). Further interpretation of the 3′-G H8 signals is complex since these signals are affected not only by Pt binding to N7 but also by shielding from the 5′-G residue.

The temperature dependence of ^{1}H NMR spectra of single-stranded oligomers containing Pt cross-linked GpG moieties is interesting. For example, broad 3′-G H8 signals have been observed for most of the single-stranded platinated oligomers.[9b-f] For d(TCTCGGTCTC)-*cis*-Pt(NH_3)$_2$, this phenomenon was observed on decreasing the temperature from 70 to 20 °C.[9f] As yet, the reasons for this line broadening have not been conclusively established. One possible explanation could be that two forms exist in a conformational equilibrium involving a change in sugar pucker, base stacking, H bonding, or a combination of these effects. Raising the temperature could favor one of the forms.

An N conformation of the 5′-G ribose moiety has been indicated for d(GG)-*cis*-Pt(NH_3)$_2$,[9a] d(CGG)-*cis*-Pt(NH_3)$_2$,[9b] d(TGGCCA)-*cis*-Pt(NH_3)$_2$,[9d] and d(ATGG)-*cis*-Pt(NH_3)$_2$,[9e] by a small $J_{1'-2'}$ value of ca. 0 to 0.7 Hz.[29] This conformation has also been indicated for d(TGGT)Pt(en), where the 5′-G H1′ signal was observed as a doublet with $J_{1'-2'}$ < 0.5 Hz. The values for $J_{1'-2'}$ of the other three ribose moieties (ca. 5–7 Hz) are consistent with predominantly S type configuration.[29] The 5′-G H1′ signals for d(CGG)-*cis*-Pt(NH_3)$_2$ and d(ATGG)-*cis*-Pt(NH_3)$_2$, clearly doublets at higher temperature, shifted upfield and broadened when the temperature was lowered.[9e] For d(ATGG)-*cis*-Pt(NH_3)$_2$ this signal was broadened to the base line by 35 °C. A similar temperature effect was observed with d(TGGT)Pt(en); however, the 5′-G H1′ signal was still observed even at 10 °C (Figure 8 and supplementary Figure S3). For d(ATGG)-*cis*-Pt(NH_3)$_2$, this phenomenon was attributed to a change in conformation, possibly due to a rotation of the d(GpG)-*cis*-Pt(NH_3)$_2$ moiety around the TpG linkage.[9e]

Since this temperature effect on the H1′ signal was not observed for d(TGGCCA)-*cis*-Pt(NH_3)$_2$,[9d] it was suggested that the presence of more than one base on the 5′ side of the platinated d(GpG) moiety may be required for such conformational equilibria.[9e] Since we have observed this phenomenon with d(TGGT)Pt(en), this suggestion seems unlikely. In an attempt to induce this conformational change by alternative means, we increased the salt concentration and added MeOH (in separate experiments) to solutions of d(TGGT)Pt(en). No change of the 5′-G H1′ signal was observed, indicating that this conformational change probably results from an intramolecular interaction.

At 5 °C, it was found that the bases of the 3′-G and 3′-T of d(TGGT)Pt(en) stack, apparent from NOE cross peaks between the 3′-G H2″ and 3′-T H6 signals. The observation of cross peaks between the 5′-T H6 and H5′,5″ signals but not between signals of the 5′-T and 5′-G residues indicates a high degree of rotational freedom of the 5′-T. In contrast to d(TGGT)Pt(en), no internucleotide NOE cross peaks were observed between the adjacent 3′-G and 3′-T residues of d(TGGT)-*cis*-Pt($MeNH_2$)$_2$. For the latter species, no cross peaks were observed between 5′-T and 5′-G. Thus, the NOE results do not provide insight into the structural relationship between the bases, except to indicate that the bases are not stacked significantly on the 200–500-ms time scale, which would lead to cross peaks.

Increasing the temperature of solutions of platinated oligomers should decrease stacking interactions and could affect H bonding of the Pt amine ligand to a phosphate group. Good quality spectra were obtained at 5 °C with d(TGGT)Pt(en), whereas other systems with at least one 5′-nucleotide often have broad spectra below 35 °C. For d(TGGT)Pt(en), an increase in temperature caused a slight downfield shift of the 5′-G H8 signal (supplementary Figure S6). This deshielding could result from decreased H bonding or elimination of the weak stacking at 5 °C, which escaped detection by NOE methods. No temperature effects were observed for the 5′-G H8 signal of d(TGGT)-*cis*-Pt($MeNH_2$)$_2$ implying, perhaps, not only an absence of stacking of the 5′-T residue but also a weaker H bond of the phosphate group to the bulky $MeNH_2$ ligand. An upfield shift of the 5′-G H8 was observed with d(GGTT)Pt(en) as temperature was increased (supplementary Figure 6).

This shift of the 5′-G H8 occurs without a 5′ neighboring base. Likewise, a very large upfield shift of ca. 0.5 ppm is observed for the 3′-G H8 signal on raising the temperature of d(CGG)-*cis*-Pt(NH_3)$_2$ solutions from 5 to 75 °C.[9b] The stacking of the 5′-C with the 5′-G is decreased over this temperature range, as indicated by an upfield shift of the 5′-G H8. Thus, although more detailed conformational analyses of platinated oligonucleotides can be obtained from ^{1}H NMR studies, the factors influencing the ^{1}H chemical shifts are difficult to decipher. As discussed previously, th factors that affect the aromatic ^{1}H NMR signals of platinated oligonucleotides include (1) coordination of the bases to the Pt drugs, (2) relative orientation of the bound G residues to each other and to their respective sugars, (3) anisotropy of adjacent bases, and (4) proximity of phosphate groups. For longer oligomers the number of signals is increased substantially. In addition, downfield-shifted aromatic signals have been observed in the ^{1}H NMR spectra for Pt adducts of oligonucleotides that do not contain a GG moiety cross-linked by Pt, such as d(TGGT) + *trans*-Pt(NH_3)$_2$$Cl_2$ (Figure 2).

^{31}P chemical shifts are influenced predominantly by phosphate bond and torsion angles and are relatively insensitive to base sequence, and concentration. In other studies[8] and this study, nontransient downfield ^{31}P NMR signals of platinated oligonucleotides were observed only for the *cis*-PtA_2Cl_2 adducts that contain a GpG moiety (Figures 9 and 10). The ^{31}P NMR studies provide an insightful view of changes about the GpG moiety of longer oligomers after treatment with Pt drugs and provide a useful and additional NMR spectroscopic method for assessing the interactions of drugs with DNA. 2D NMR methods are becoming increasingly useful as they allow correlations via homonuclear and heteronuclear scalar interactions, dipolar interactions (which give internuclear distances), and separation of overlapping signal components in complex spectra. Together these methods have provided results consistent with H bonding between the 5′-phosphate moiety and an NH group on the amine ligand, but further studies may be needed to conclusively establish such interactions in solution.

Acknowledgment. Support for this work by NIH Grant GM29222 and a loan of K_2PtCl_4 from Matthey-Bishop, Inc., are greatly appreciated. We also thank Kai-liu Shao, Joel Hoskins, and Judy Regan for technical assistance.

Supplementary Material Available: Figures S1–S8, showing entire plots of the HOHAHA and COSY data of d(TGGT)-*cis*-Pt($MeNH_2$)$_2$, ^{1}H NMR spectra of the reaction of d(pGGTT) with Pt(en)Cl_2, temperature dependence of the base and H1′ protons of d(TGGT)Pt(en), of the 3′- and 5′-G H8 signals, and of the GpG ^{31}P signals of selected Pt adducts of the oligonucleotides, and the pH dependence of the ^{31}P signals of d(pGGTT)Pt(en) (8 pages). Ordering information is given on any current masthead page.